A Theory of Local and Global Processes Which Affect Solar Wind Electrons 1. The Origin of Typical 1 AU Velocity Distribution Functions—Steady State Theory

JACK D. SCUDDER

NASA/Goddard Space Flight Center, Laboratory for Extraterrestrial Physics Greenbelt, Maryland 20771

STANISLAW OLBERT

Physics Department, Center for Space Research, Massachusetts Institute of Technology Cambridge, Massachusetts 02139

A new detailed first principle kinetic theory for electrons is presented which is neither a classical fluid treatment nor an exospheric calculation. This new theory illustrates the global and local properties of the solar wind expansion that shape the observed features of the electron distribution function f_e, such as its bifurcation, its skewness, and the 'differential' temperatures of the thermal and suprathermal subpopulations. Our approach starts with the Boltzmann equation and retains the effects of Coulomb collisions via a Krook collision operator without recourse to wave-particle effects. We conclude that Coulomb collisions determine the population and shape of f_e in both the thermal ($E < kT$) and suprathermal ($E > kT$) energy regimes. We find that electrons with $E > 7kT$ constitute a special subpopulation of the suprathermals, insofar as Coulomb collisions are concerned; these we call 'extrathermals.' The electrons in the thermal portion of f_e have undergone ~10–20 Coulomb collisions for cumulative momentum transfer en route to the observer at 1 AU; this population is thus more removed from the properties of coronal electrons than the suprathermal population. This latter group retains a strong memory of coronal conditions, since they have undergone only a few momentum transfer collisions. The thermal population is most nearly in collisional contact with the local dynamics (compressions, rarefactions, etc.) of the solar wind. The suprathermal portion of f_e is determined by Coulomb collisional interactions with the distribution of solar wind material on radial scale of the heliopause itself. In this respect the suprathermal portion of f_e is found to be responsive to the consequences of the global dynamics of the solar wind expansion. We find that this subpopulation is an attenuated vestige of collisional populations deep in the corona (1.03–10 R_S) which has been redistributed via Coulomb multiple pitch angle scattering on magnetically open field lines. The suprathermal particles moving toward the sun are computed to be observed as a result of Coulomb-collision-induced backscattering at larger (1–10 AU) heliocentric distances than that of the observer. Based on this theoretical picture, quantitative estimates for the partition of thermal and suprathermal phase density, the break in the velocity distribution, and the magnitude of the skewness (heat flux density) agree well with those typically observed near 1 AU. These calculations predict that the extrathermal fraction of the phase density, the extrathermal temperature, and the net heat flux density carried by electrons should be anticorrelated with the local bulk speed in quasi-steady-state flows and that the radial variation of extrathermal temperature inside 1 AU should be essentially independent of heliocentric distance. Our work also shows that the observation of suprathermal particles cannot be taken as a priori evidence for in situ wave particle interaction(s), since we can theoretically calculate a suprathermal population of solar wind electrons at 1 AU by assuming wave-particle interactions are not present anywhere in the heliospheric cavity; the combination of inhomogeneity and the Coulomb 'window' above $E^* = 7kT_c$ naturally gives rise to this leakage of nonlocal collisional populations in superposition with local collisional populations. This work suggests that the local cause and effect precept which permeates the physics of denser media must be relaxed for electrons in sparse and radically inhomogeneous plasmas such as those found in the solar wind between the lower corona and the interstellar medium. The local form of transport laws and equations of state (e.g., $Q = -\kappa\nabla T$, $P = NkT$), which are familiar from collision-dominated plasmas, must be replaced with global relations that explicitly depend on the relative position of the observer to the boundaries of the system.

1. INTRODUCTION

In this paper (paper 1) we suggest that the typical velocity distribution function of solar wind electrons in a quasi-steady flow is shaped primarily by the properties of Coulomb collisions and the 'smooth' macroscopic forces implied in the solar wind expansion. Following a straightforward mathematical procedure, we illustrate how some of the controlling effects, both local and global, are reflected in the in situ observations. In companion papers we discuss (paper 2) the consequences of this theory and its comparison with known experimental facts, (paper 3) the impact of this approach on the question of transport phenomena (such as heat flows, viscous effects, etc.) in the heliosphere and the relation of the current formulation to canonical transport methods, and (paper 4) a mathematically more rigorous formulation of the problem discussed in paper 1.

Historically, theoretical treatments for solar wind electrons have variously approximated the electrons either (1) as part of a one-fluid model of the wind [*Parker*, 1963], (2) as a separate fluid interacting via Coulomb (local) momentum transfer with the ions [*Hartle and Sturrock*, 1968], or (3) as an exospheric ('collisionless') population above some radial distance (called the 'baropause' or 'exobase') (*Jockers* [1970], and independently by *Lemaire and Scherer* [1971]).

Paper number 9A0280.
0148-0227/79/009A-0280$01.00

Ogilvie and Scudder [1978] showed with in situ measurements between 0.45 and 0.9 AU (*Feldman et al.* [1978] at 1 AU concur) that the local mean free path λ for scattering of thermal electrons via Coulomb effects was less than the conventionally defined scale height H, implying that Coulomb effects could not be neglected even within 1 AU. Therefore the propagation of electrons neglecting particle-particle collisions from a baropause to the in situ observer is not the correct kinetic description of the solar wind expansion insofar as electrons are concerned. However, *Ogilvie and Scudder* [1978] indicated that λ/H was not very small in comparison with unity, indicating that the fluid treatment was not justified either. It is therefore fruitful to explore the effects of Coulomb collisions in shaping the in situ distributions, by not making either the exospheric or fluid approximation.

It has been previously realized that the Knudsen number $K = \lambda/H$, as determined a posteriori from fluid solar wind models, can be so large in some regions as to invalidate the conduction law used to obtain the solution. Until recently this inconsistency has been thought to be relatively unimportant, since K was thought to be small and the solar wind expansion hydrodynamic in the initial acceleration phase and somewhat irrelevant once the flow had become supersonic and momentum dominated [e.g., *Griffel and Davis,* 1969]. However, the discussion of *Durney and Hundhausen* [1974], *Durney and Pneuman* [1975], *Kopp and Orrall* [1977], *Singer and Roxburgh* [1977], and *Lemaire* [1978] highlight the renewed criticism of using collision-dominated transport coefficients (small Knudsen number approximation) for the solar wind even within the strong initial subsonic acceleration over coronal holes. The last reference emphasizes that exospheric theory ($K \rightarrow \infty$) could also be improved with the added effects of collisions.

Since the original work of *Montgomery et al.* [1968] it has been experimentally established that the electron velocity distribution function $f_e(\mathbf{v})$ was not a simple Maxwellian. The reported phase density in the suprathermal regime significantly exceeded that predicted by the best fit (bi-) Maxwellians to the thermal regime of f_e. The thermal and suprathermal subpopulations of the solar wind electrons were subsequently named the 'core' (or cold) and 'halo' (or hot) components, respectively, by *Feldman et al.* [1975], who modeled the electron phase density as a superposition of mildly anisotropic, relatively drifting, bi-Maxwellians with different temperatures, densities, and bulk speeds. Recently, *Rosenbauer et al.* [1976, 1977] showed that a narrow (~20°) magnetic-field-aligned 'strahl' (or ray) can occasionally be observed in the suprathermal phase density.

The observations of *Ogilvie and Scudder* [1978] (*Feldman et al.* [1978] confirmed) also indicated that the local scattering mean free path (mfp) for halo electrons was long in comparison with the local density scale height. In the customary sense of the word, the halo particles were locally 'collisionless.' Nevertheless, there is some weak, omnipresent, unavoidable Coulomb interaction with the thermal plasma. The suprathermal electron population of fixed energy is generally observed in all octants of velocity space with comparable phase density [*Montgomery et al.,* 1968; *Scudder,* 1970; *Ogilvie et al.,* 1971]. *Feldman et al.* [1974] have suggested that wave-particle interactions are the reason for their 'ubiquity.'

The theory of electron-wave interactions as contrasted with instability onset calculations [*Forslund,* 1970; *Gary et al.,* 1975; *Singer and Roxburgh,* 1977] is not well developed. Since the original suggestion of *Parker* [1962], wave-particle interactions [*Pines and Bohm,* 1952] have been invoked to reconcile the predictions of collisionless plasma orbit theory with the observed anisotropy characteristics of ions [*Neugebauer and Snyder,* 1966] and electrons [*Feldman et al.,* 1974]. However, the important issue not to lose sight of is the relative importance of wave-particle and collisional effects as emphasized by *Hundhausen* [1968]. In this connection it is important to emphasize from the beginning that collisional frequencies are strong functions of particle speeds and that real frequencies associated with collective instabilities should be compared with the relevant speed regime collisional frequency from which the 'wave' derives its free energy.

The origin of the spectrally distinguishable halo subpopulation of solar wind electrons was initially suggested by *Ogilvie and Scudder* [1978] when they extrapolated the electron measurements made by the Mariner 10 plasma science experiment of the radial variations ($0.45 < R < 0.9$ AU) of the core and halo (differential) 'temperatures':

$$T = -\frac{1}{k_B}\left(\frac{d \ln f}{dE}\right)^{-1}$$

to determine the radial positions where these best fit variations predicted a common temperature. Depending on the assumptions, this zone of common (differential) temperature was between 2 and 15 R_S. The suggestion of that paper was that a fractionation process of the antecedents of halo and core subpopulations had begun in this radial range. The subsequent approximate experimental inference of the origin of the strahl portion of the halo in very high speed flows [*Feldman et al.,* 1978] confirms the approximate location of this fractionation process.

We shall demonstrate below, by explicit calculation, that the suprathermal electrons with $E > 7kT_c$ observed near 1 AU are an attenuated vestige of collisional populations deep in the corona (1.03 to ~15 R_S) which have been redistributed via Coulomb multiple small angle pitch angle scattering. The cumulative spatially integrated effects of Coulomb pitch angle scattering are sufficient to explain the observed proportion of suprathermal electrons both fore and aft along the local magnetic field. We show that the halo population is shaped by the spatially integrated nonlocal (i.e., global) features of the heliospheric cavity—such as its size, its large-scale magnetic topology, and the spatial variation of its contents—especially near the extremities of the solar wind expansion. In this latter sense, in situ electron observations allow remote observations of important regimes of the solar wind expansion which are presently not accessible.

Terminology

It is appropriate to comment on our use of the word 'suprathermal' and other new terms we wish to use in the remainder. From the latin supra, meaning above, the clear intent of 'suprathermal' is to delineate those particles with energy larger than $E = k_BT$ (where k_B is Boltzmann's constant), which is the kinetic energy of a particle moving with the most probable speed. For electrons we operationally assign the 'core' temperature to delineate the most probable speed. For particles with $E > k_BT_{\text{core}}$ it is consonant with the literature to discuss this entire range as the suprathermal domain. In paper 2 we shall show that electrons with kinetic energy $E \gtrsim 7kT_c$ are a special subset of the suprathermals insofar as Coulomb collisions are concerned. These particles have energies sufficiently beyond those of the thermal electrons as to have a minimal local interaction with them. Moreover, as is shown below, these extrathermals have also come from substantially beyond the

position of the observer. For clarity we have labeled this group as the 'extrathermals,' noting that extra means beyond in Latin. The particles of intermediate energies ($1 < E/k_BT_c \lesssim 7$) are most suitably labeled as 'transthermals' (trans meaning across) for two reasons: (1) they bridge the energy interval between subthermal and extrathermal populations and (2) these electrons are populated from collisional antecedents with nonnegligible contributions distributed across a substantial portion of the heliosphere. We shall use the term subthermal, thermal, transthermal, and extrathermal to delineate specific energy regimes in the above sense; when we do not wish to distinguish between transthermal and extrathermal, we will use the word suprathermal. As is discussed below, we do not regard the term 'suprathermal' as being synonymous with that suggested by *Parker and Tidman* [1958] for particle populations generated by local Fermi mechanism and/or betatron action.

Organization

We outline the structure of this paper to orient the reader. The theoretical transport problem is posed in a formulation section (section 2). We next discuss formal solutions (section 3), which give the flavor of the explicit solutions whose details can only be obtained after the mathematical considerations (section 4) and implementation (section 5). The outcome of two 'realizations' of the formal solution are given in a results section (section 6), followed by a discussion, prediction, and conclusion section (section 7).

2. FORMULATION

For the present we desire to estimate in the simplest possible fashion the consequences of a physically complete picture of Coulomb collisions as they would shape and determine in situ observations of electrons in the solar wind without considering wave-particle scattering. The advantages of the present formulation include simplicity and ease of physical interpretation. Estimates of the importance of Coulomb interactions can be made simply by evaluating integrals rather than by solving partial differential equations. In this approach the solution of the scattering problem is available in closed form and has a conceptually simple interpretation with predictions which can be checked against the variability and correlations of local observations; it also allows definite predictions at other heliocentric distances.

The basic equation governing our discussion is the Boltzmann equation

$$\frac{df}{dt} \equiv \frac{\partial f}{\partial t} + \mathbf{v} \cdot \frac{\partial f}{\partial \mathbf{x}} + \frac{\mathbf{F}}{m} \cdot \frac{\partial f}{\partial \mathbf{v}} = \left.\frac{\delta f}{\delta t}\right|_{\text{collison}} \tag{1}$$

where the symbols have the usual meaning: f is the particle distribution function at coordinates $(\mathbf{r}, \mathbf{v})$ in the phase space, $\mathbf{F}$ are the 'smooth' forces experienced by the particle, and $\delta f/\delta t$ is the Boltzmann collision term which is given explicitly by

$$\left.\frac{\delta f}{\delta t}\right|_{\text{collision}} = -n\left[\int d\mathbf{v}_1 \int d\Omega\ \frac{d\sigma}{d\Omega} f(\mathbf{v})|\mathbf{v} - \mathbf{v}_1| f(\mathbf{v}_1) - \int d\mathbf{v}_1' \int d\Omega'\ \frac{d\sigma'}{d\Omega'} f(\mathbf{v}')|\mathbf{v}' - \mathbf{v}_1'| f(\mathbf{v}_1')\right]$$

where $\mathbf{v}$, $\mathbf{v}_1$ are the precollision velocities and the primed $\mathbf{v}'$, $\mathbf{v}_1'$ are the postcollision velocities.

The first term of $(\delta f/\delta t)|_{\text{collision}}$ determines the loss rate of f from $(\mathbf{r}, \mathbf{v})$ as a result of the scattering of particles with precollision velocities $\mathbf{v}'$, $\mathbf{v}_1'$. The second term of the collision term describes the local replenishment of phase density at $(\mathbf{r}, \mathbf{v})$ as a result of scattering into the local phase space volume element. The differential scattering cross section is given by $d\sigma/d\Omega$.

For purposes of the estimates in this paper we shall approximate the collision term in the Boltzmann equation in the form proposed by *Bhatnagar et al.* [1954] and extended by *Gross and Krook* [1956]; this approach is known variously as the BGK, Krook, or relaxation time approximation (cf., e.g., *Reif* [1965]); the approximation is mathematically exceptionally simple and physically not only instructive but has been shown to be quite satisfactory in other comparable physical situations.

As was clearly realized by *Gross and Krook* [1956], this approximation is not restricted to the small mean free path transport case which leads to the Chapman-Enskog type analysis. Therefore our use of the relaxation time approximation is not synonymous with the short mean free path limit ($v\tau/L \ll 1$, where v is the particle speed and L is a characteristic scale length of the gradients).

The inadequacies and simplicity of the Krook model are well known [cf. *Gross and Krook,* 1956; *Rawls et al.,* 1975]. As it is currently used, it does not strictly conserve density, momentum, or energy. As the scattering time τ we introduce is that for 90° cumulative pitch angle deflection, and as $(\delta f/\delta t)|_{\text{Coulomb}}$ is more complicated than this, and as $(\delta f/\delta t)|_{\text{Krook}}$ depends on an a priori guess of f_k, this approximation cannot be a priori made to describe with equal fidelity the true nature of the Coulomb interaction between 'test' electrons of all energies and the background plasma. Without the use of a more sophisticated Fokker-Planck collision operator of the type suggested by *Rosenbluth et al.* [1957] (the RMJ model), it seems unwarranted to pursue the rigors, within the Krook model, of conserving quantities determined by various weighted velocity space averages over the entire velocity distribution function. Nevertheless, the current approximation behaves for low (subthermal) test electrons in the same qualitative manner as the correct treatment (cf. section 6), while also allowing estimates to be made of scattering effects at higher (suprathermal) energies. The present analysis already yields information that illustrates some global features of electron transport in an inhomogeneous plasma that is fully ionized.

Consider at some point $\mathbf{r}$ the (unknown) electron phase density $f(\mathbf{r}, \mathbf{v}, t)$. Then in Krook's approximation, f obeys the equation

$$\frac{df}{dt} = -\frac{[f - f_k(\mathbf{r}, \mathbf{v})]}{\tau(\mathbf{r}, \mathbf{v})} \tag{2}$$

By comparing the structure of (2) with that of (1) we obtain the correspondences:

$$\tau = \left(n \int d\mathbf{v}_1 \int d\Omega\ \frac{d\sigma}{d\Omega} f(\mathbf{v}_1)|\mathbf{v} - \mathbf{v}_1|\right)^{-1}$$

$$f_k = \frac{n^2\left(\int d\mathbf{v}_1' \int d\Omega'\ \frac{d\sigma'}{d\Omega'} f(\mathbf{v}') f(\mathbf{v}_1')|\mathbf{v}' - \mathbf{v}|\right)}{\left(\int d\mathbf{v}_1 \int d\Omega\ \frac{d\sigma}{d\Omega} f(\mathbf{v}_1)|\mathbf{v} - \mathbf{v}_1|\right)} \tag{3}$$

where it is clear that f_k and τ are functionals of the unknown distribution function.

The Krook approximation to the collision operator $\delta f/\delta t$ not only retains the formal structure of the Boltzmann operator, but allows, by a judicious choice of $f_k(\mathbf{r}, \mathbf{v})$, a linearization of the full transport equation that is very instructive.

We shall now examine some properties of $(\delta f/\delta t)|_{\text{Krook}}$ to understand the role of $f_k(\mathbf{r}, \mathbf{v})$ in this approximation.

In the special circumstance of a uniform system where electric fields and gravity are unimportant and the distribution function is perturbed isotropically in the proper frame velocity space and uniformly in configuration space and τ is a simple constant independent of space or velocity, then (2) reduces to

$$\frac{df}{dt} = \frac{\partial f}{\partial t} = -\frac{(f - f_k)}{\tau} \tag{4}$$

The solution of (4) is

$$f(|\mathbf{v}|, t) = f(|\mathbf{v}|, t_0) + [f_k(|\mathbf{v}|) - f(|\mathbf{v}|, t_0)] \cdot \left[1 - \exp\left(-\frac{(t - t_0)}{\tau}\right)\right] \tag{5}$$

where for this example τ is assumed independent of time t. From this example it is clear that f_k should be interpreted as a final state of the relaxation process. The temporal relaxation given by (5) is caused by $(f - f_k)|_{t_0} \neq 0$ (i.e., the departures of the initial from the final state) and by the evidence for a finite relaxation time τ.

The preceding discussion was for an extremely special situation for the Boltzmann evolution operator with a collision term approximated after the model proposed by Krook and collaborators. By contrast we require the steady state solution of (2) ($\partial f/\partial t = 0$) for the more general situation, in the expanding solar corona where there are nonnegligible forces and spatial inhomogeneities and speed-dependent collision frequency. This circumstance is far more common than the simplifying example of (5). Nevertheless, that example has been instructive in supplying insight into the meaning of f_k which may be carried over into the more general case we wish to pursue: namely, if $f(\mathbf{r}, \mathbf{v}) = f_k(\mathbf{r}, \mathbf{v})$, then this is a stationary solution of the Boltzmann equation with a Krook approximated collision operator.

The distribution $f_k(\mathbf{r}, \mathbf{v})$ represents the time-independent spatially inhomogeneous final state toward which the relaxation mechanism, with scale time τ, drives an initially perturbed distribution. Of course, f_k is not known a priori; however, using the in situ tendency for the thermal electrons to be nearly Maxwellian [*Montgomery*, 1968; *Feldman et al.*, 1975; *Ogilvie and Scudder*, 1978], we make an empirical ansatz for the final profile in zeroth-order approximation:

$$f^{(0)} = f_k(\mathbf{r}, |\mathbf{v}|) \simeq f_k^{(0)} = \frac{n(\mathbf{r})}{\pi^{3/2}(2k_B T_c(\mathbf{r})/m_e)^{3/2}} \cdot \exp\left(-\frac{m_e|\mathbf{v} - \mathbf{U}(\mathbf{r})|^2}{2k_B T_c(\mathbf{r})}\right) \tag{6}$$

which is a convected Maxwellian distribution with spatially varying density $n(\mathbf{r})$, bulk velocity $\mathbf{U}(\mathbf{r})$, and temperature $T_c(\mathbf{r})$.

The relaxation process visualized here is characterized by the familiar rate of Coulomb collisions ν_c between 'test' electrons and 'targets,' i.e., the positive ions and other ambient electrons. Recalling that $\nu_c \equiv 1/\tau$, we have (cf., e.g., *Rossi and Olbert* [1970])

$$\frac{1}{\tau} \equiv \nu_c = \frac{\nu_{ep} w_{T,e}{}^3 \mathcal{J}(w/w_{T,e})}{|\mathbf{w}|^3} \tag{7}$$

This is the rate at which phase density is scattered out of the observer's phase density element, where in cgs units

$$\nu_{ep} = \frac{n \ln [1.2 \times 10^5 (T^{1/2} T_e)/n^{1/2}]}{0.38 T_e^{3/2}} \text{ s}^{-1} \tag{8}$$

and where T is the harmonic temperature of T_e and T_p; the speed $|\mathbf{w}| = w$ is the particle speed in the proper frame. The root mean square (rms) thermal speed of species a is given by

$$w_{T,a} = (3k_B T_a/m_a)^{1/2} \tag{9}$$

The statistical effects of the thermal spread of the ambient targets is contained in the function $\mathcal{J}$ of (7), defined by

$$\mathcal{J} = \left\{\left[\text{erf}\left(\left(\frac{3}{2}\right)^{1/2}\frac{w}{w_{T,p}}\right)\left(1 - \frac{w_{T,p}{}^2}{3w^2}\right) + \exp\left(-\frac{3}{2}\frac{w^2}{w_{T,p}{}^2}\right)\left(\left(\frac{2}{3\pi}\right)^{1/2}\frac{w_{T,p}}{w}\right)\right] + \frac{1}{2}\left[\text{erf}\left(\left(\frac{3}{2}\right)^{1/2}\frac{w}{w_{T,e}}\right)\left(1 - \frac{w_{T,e}{}^2}{3w^2}\right) + \exp\left(-\frac{3}{2}\frac{w^2}{w_{T,e}{}^2}\right)\left(\left(\frac{2}{3\pi}\right)^{1/2}\frac{w_{T,e}}{w}\right)\right]\right\} \tag{10}$$

A more general form for $\mathcal{J}$ is given by *Rossi and Olbert* [1970]. In that expression, $\mathcal{J}$ is a functional of the ambient electron and ion distribution functions f_e and f_i. The expression given in (10) has been evaluated with local Maxwellians for both electrons and ions.

Brandt and Cassinelli [1966] showed the importance of the velocity dependence of the Coulomb process in providing the first exospheric calculation of the coronal expansion with a supersonic asymptotic flow state. The velocity dependence of ν implied different energy particles were 'free' at different radial distances. They used the concept of energy-dependent exobases for subsequent 'collisionless' egress from the coronal base. This solution (although using the inaccurate Pannekoek-Rosseland polarization potential) resolved the controversy between *Chamberlain* [1960] (exospheric, single exobase, solar breeze) and *Parker* [1963] (hydrodynamic, collision dominated, solar wind) that seemed to suggest that the nature of the solar expansion depended on whether one adopted a corpuscular or a continuum description of the mass loss.

3. Information From Formal Solutions

Although formal solutions are rarely directly amenable to calculation, they often compactly display the conceptual character of the more complicated explicit solutions. We proceed to give several instructive equivalent formal solutions to the Boltzmann equation, with the Krook approximated collision term, in order that the reader obtain the flavor of the more complicated explicit computational form of the solutions which we discuss in the next two sections.

The formal solution of (2) at the observer's time t is

$$f(t) = f_k(t_0) \exp[-S(t, t_0)] + \oint \exp[-S(t, t')] f_k[t']/\tau[t']\, dt' \tag{11}$$

where

$$S(t, t') \equiv \oint_{t'}^{t} \frac{dt''}{\tau[t'']} \tag{12}$$

and where the indicated path integrals $\oint$ are performed following the trajectory of a representative point of an electron in the six-dimensional phase space.

Noting that $S(t, t) \equiv 0$ and that

$$dS(t, t') = -\frac{dt'}{\tau[t']} \qquad \forall t' < t \tag{13}$$

and, with the definitions

$$S_0 \equiv S(t, t_0) \qquad \Delta S \equiv S(t, t') \tag{14}$$

(11) may be recast in a number of illuminating ways:

$$f(t) = f_k(t_0) \exp(-S_0) + \oint_0^{S_0} \exp(-\Delta S) f_k[t'(\Delta S)]\, d(\Delta S) \tag{15}$$

which, upon integration by parts, becomes

$$f(t) = f_k(\Delta S = 0) + \oint_0^{S_0} \exp(-\Delta S) \left\{\frac{df_k[t'(\Delta S)]}{d(\Delta S)}\right\} d(\Delta S) \tag{16}$$

or, equivalently,

$$f(t) = f_k(\Delta S = 0) + \oint_{f_k(\Delta S=0)}^{f_k(\Delta S=S_0)} \exp(-\Delta S[f_k(t'[\Delta S])])\, d[f_k] \tag{17}$$

Equations (11) and (15)–(17) are all equivalent, highly compact, formal answers to the transport question posed at the beginning of this section. Before discussing the content of these solutions, we need a physical interpretation of the quantity ΔS.

The quantity ΔS is the collisional analog of the optical depth of radiative transfer. We will refer to this intrinsically nonnegative quantity as the collisional depth of the observer relative to the source. It is a cumulative ($\oint$) counter of collisional cycles ($1/\tau$) experienced by the representative point of a particle in the phase space element during its motion [at t''] from the departure at t' to the present, at t. The quantity $\exp(-\Delta S)$ which occurs throughout these equations can be thought of as a normalized survival probability upon transiting the collisional depth ΔS.

To appreciate some of the essential physics of the nonlocal terms of (15)–(17), we must discuss electron kinematics and the use of collisional depths and boundary conditions.

The most probable speed of the electrons throughout the solar cavity is many times the typical solar wind speed. Hence nearly all electrons are kinematically able to transport information in both directions along a magnetic tube of force. Because of this mobility it is by no means obvious where the electron has been in the solar system preceding its detection. For electrons the in situ observation from a given collisional depth ΔS of the velocity distribution function is a synthesis of particles and information coming from both fore and aft along the local magnetic field.

Collisional depths, like their optical counterparts, are intrinsically nonnegative. When considering contributions to the local distribution from a given collisional depth ΔS, we are considering contributions from particles which at time $t' < t$ were either inside or outside the observer's radial position (cf. Figure 1). A corollary to these comments is that all electrons observed at $\mathbf{r}$ at time t probably did not leave the sun at, or even nearly at, the same time, t_0, in the past. Rather, the observed $f(\mathbf{r}, \mathbf{v}, t)$ is the superposition (i.e., an integral) of all the surviving probability densities whose representative electrons have accessible trajectories to the current observer's point $(\mathbf{r}, \mathbf{v})$ in the full six-dimensional phase space. Depending on the collisional depth and its variation with energy and pitch angle and the temporal boundary conditions at the source layers, $f[\Delta S(t')]$, the observed distribution will be more or less reflective of the coronal or collisional conditions along the local observer's magnetic tube of force.

Thus (15) has the following physical content: the velocity probability distribution $f(\mathbf{r}, \mathbf{v}, t)$ observed at time t is the sum of two parts. The first, on the right-hand side of (15), the so-called boundary term, is the contribution to the currently observed f that has survived extinction from the space time boundary of the system to the observer. The second contribution is the folded sum ($\oint$) over all intermediate collisional depths $0 < \Delta S < S_0$ of $f_k[t'(\Delta S)]$, weighted by their respective attenuations, $\exp(-\Delta S)$, between source and observer. (Remember that for a given ΔS there are two positions along the tube of force from which $\oint$ has contributions: one effective location outside, one inside that of the observer (cf. (35*a*), (35*b*)).)

Equation (16), although entirely equivalent to (15), gives a slightly different physical description to the observed distribution: the first term on the right-hand side of (16) is the 'local' term, since it is the source distribution at collisional depth zero from the observer; the second term describes the corrections to the local sources as properly attenuated signals of the variability of the nonlocal distribution with differential changes in the collisional depths from the observer. This formal solution (16) is the point of departure for our discussion of paper 3. Equation (17) follows from (16) by change of variables. Note from (17) that if the system is everywhere homogeneous, then $f_k(\Delta S = S_0) = f_k(\Delta S = 0)$ and (17) collapses to $f = f_k(\Delta S)$. This is the special case of thermodynamic equilibrium. Conversely, if, for example, the electron temperatures at $\Delta S = S_0$, 0 are not equal, then the $\oint$ term of (17) is not equal to zero (since the integrand is positive definite). The corrections to the local population ($f_k(\Delta S = 0)$) that are observed are the signatures of spatial inhomogeneities of f_k in the system.

From these formal solutions we see that the local observations represent a superposition of phase densities displaced from the observer ($\Delta S \neq 0$) folded with the probability that these phase space elements can 'survive' between their collisional origin and the observer. This is a mathematical statement of the dynamical accessibility of the electrons to the observer. In order to evaluate these solutions further, some mathematical arguments are required.

4. Mathematical Interlude

The discussion which follows pertains to the directions of information flow to a given point in $(\mathbf{r}, \mathbf{v})$ space.

In order to 'reassemble' the Lagrangian style solutions available from (15) for the evolution of different phase space elements into an Eulerian description for the velocity distribution at a given position r, as $t \to \infty$, we must categorize classes of trajectories in steady state which are accessible to the position of the observer.

In this connection it is important to note that electrons of energies less than ~10 keV have gyroradii which are extremely small by astrophysical scales at any heliospheric distance. It is thus difficult for solar wind electrons to drift perpendicular to the magnetic lines, and therefore excepting the effects of collisions, the electron guiding centers reside on the line of force on which they were initially injected. Although collisions can enhance crossfield diffusion, this effect is negligible at $r_0 = 1$ AU, since $D_\perp/D_\parallel \sim 10^{-16}$, where $D_{\perp,\parallel}$ are the collisionally

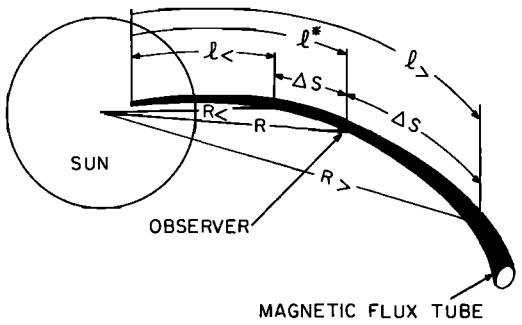

Fig. 1. Idealized magnetic topology. For electrons the arc length, time coordinates (l^*, t^*) are synonymous with the space time position (r^*, t^*). Note that script els of the figure have been typeset in the text as lower case italic els.

induced diffusion coefficients transverse and longitudinal to the local magnetic field. This ratio scales as

$$\frac{D_\perp/D_\parallel|_R}{D_\perp/D_\parallel|_{R_0}} = \left[\left(\frac{T(R)}{T(R_0)}\right)^{3/2}\frac{N(R_0)B(R)}{N(R)B(R_0)}\right]^2 \tag{18}$$

This ratio is approximately 10^{-24} in the corona and is small throughout the heliosphere. Thus the history and future of the guiding center motion of electrons in the solar wind is intrinsically one dimensional and determined by the topology of one given line of force. Nevertheless, the guiding center motion does not behave like collisionless theory would indicate; rather, there are collisional modifications within this one-dimensional motion. Accordingly, we adopt an Archimedian magnetic topology (Figure 1) after Parker and use the arc length l^* along the given lines of force interchangeably with the corresponding radial distance r^* of the observer from the sun's center. As far as the motion of electrons is concerned, the history and future of the electron trajectory is along the given tube of force that passes through the observer's position at (r^*, t^*). The discussion which follows assumes the fluid flow to be time independent in the corotating frame. In paper 2 we will discuss to what extent the violation of these assumptions will change our results.

We introduce some diagrammatic methods for listing the types of particle trajectories that can gain access along a single tube of force to the observer's phase space volume element $d\mathbf{r}d\mathbf{v}$ about ($\mathbf{r}^*$, $\mathbf{v}^*$). In Figure 2 we illustrate representative trajectories of four types of contributions to the locally observed distribution function f. There are two classes of contributions to the forward pitch angle portion, f^+, of f (Figure 2*a*): (1) those contributions with ultimate 'source' in a collisional distribution outside ($l_>$) of the position of the observer (l^*) for times ($t_>'$) prior to the time (t^*) of detection and (2) those contributions from inside ($l_<$) the position of the observer at times $t_<'$ prior to the detection time t^*. (Refer to Figure 1 for the location of $l_<$ and $l_>$.) These same two categories apply to the available contributions to the aft, f^-, pitch angle distribution (Figure 2*b*).

The first group of accessible trajectories in Figure 2*a* are those which leave the source point (1) with space time coordinates ($l_<$, $t_<'$) and arrive at the observer's point (0) with coordinates (l^*, t^*) without having been pitch angle backscattered; i.e., dl/dt is never zero between $l_<$ and l^*. We introduce a special symbol for this generic type of collisional depth between source and observer, δS_{10}. Note, however, that in general $\delta S_{lm} \leq \Delta S_{lm}$ for general positions labeled l, m. If we desire to consider contributions from all collisional depths, even from this restricted type of contribution from this one source layer, ($t^* - t_<'$) must be allowed to range from 0 to infinity in order to compute these contributions properly. By definition then the probability P of transiting δS_{10} is given by $P_{10} = \exp(-\sigma S_{10}) \equiv P^{(0)} \exp(-\delta S_{10})$, which defines $P^{(0)} \equiv 1$.

Another example of this group are those trajectories P_{20} which are like $2 \to 1 \to 0$ in Figure 2, characterized by having one stochastically induced turning point ($dl/dt = 0$) between source layer and observer. Collisional depths are additive (cf. (12)), and therefore

$$\Delta S_{20} = \Delta S_{21} + \Delta S_{10} \equiv \Delta S_{21} + \delta S_{10} \tag{19}$$

Therefore $P_{2\to 0} = \exp(-\Delta S_{21}) \exp(-\delta S_{10}) \equiv P^{(1)} \exp(-\delta S_{10})$, which defines $P^{(1)}$. Clearly, ΔS_{20} may also range from 0 to infinity, either because ΔS_{21} and/or ΔS_{10} do. Similar considerations yield

$$\Delta S_{30} = \Delta S_{32} + \Delta S_{21} + \delta S_{10} \tag{20}$$

with any and/or all the quantities having infinite range. Higher-order quantities of these types can readily be seen to be more turning points between the time the particle left the source and reached the observer.

We shall assume for paper 1 that elastic pitch angle scattering is more efficient than inelastic scattering in backscattering electrons everywhere in the heliosphere. In the present context, elastic scattering implies that the test electron undergoes a pitch angle change with no simultaneous loss of proper frame kinetic energy; inelastic scattering implies a loss of proper frame kinetic energy while the pitch angle is changing.

The dominant fraction of momentum transfer collisions for test electrons is off of fully ionized ambient ions. This is an essentially elastic process. Test electrons scatter off of other background electrons both elastically and inelastically.

With the above provisos we shall proceed on the assumption of exclusively elastic Coulomb backscattering. By simple geometrical considerations and the assumed stationarity of the Hamiltonian, we obtain (see appendix for details)

$$\Delta S_{m,m+2} = 2\delta S_{m*} \tag{21}$$

where δS_{m*} is the collisional depth between the mth reference point and the next turning point on the trajectory as time increases.

Therefore the integrated probability $P^{(1)}$ that a particle leaves (l_m, t_m) and returns to ($l_n = l_m$, t_n), along the tube of force of infinite length, after only one turning point is

$$\begin{aligned} P^{(1)} &= \int_0^\infty \left[\begin{array}{c}\text{probability of survival}\\ \Delta S = 0 \to \Delta S = \delta S_{1*}\end{array}\right] \\ &\quad \cdot\left[\begin{array}{c}\text{probability of reflection}\\ \text{at } \Delta S = \delta S_{1*}\end{array}\right] \\ &\quad \cdot\left[\begin{array}{c}\text{probability of survival}\\ \delta S_{1*} \to \delta S_{1*} + \delta S_{*_2}\end{array}\right] d(\delta S_{1*}) \\ &= \int_0^\infty \exp(-\delta S_{1*})\cdot[1 - \exp(-\delta S_{1*})] \\ &\quad \cdot\exp(-\delta S_{*_2})\, d(\delta S_{1*}) \end{aligned} \tag{22}$$

Using (21), we obtain

$$P^{(1)} = \int_0^\infty d(\delta S_{1*}) \exp(-2\delta S_{1*})[1 - \exp(-\delta S_{1*})] = \frac{1}{6} \tag{23}$$

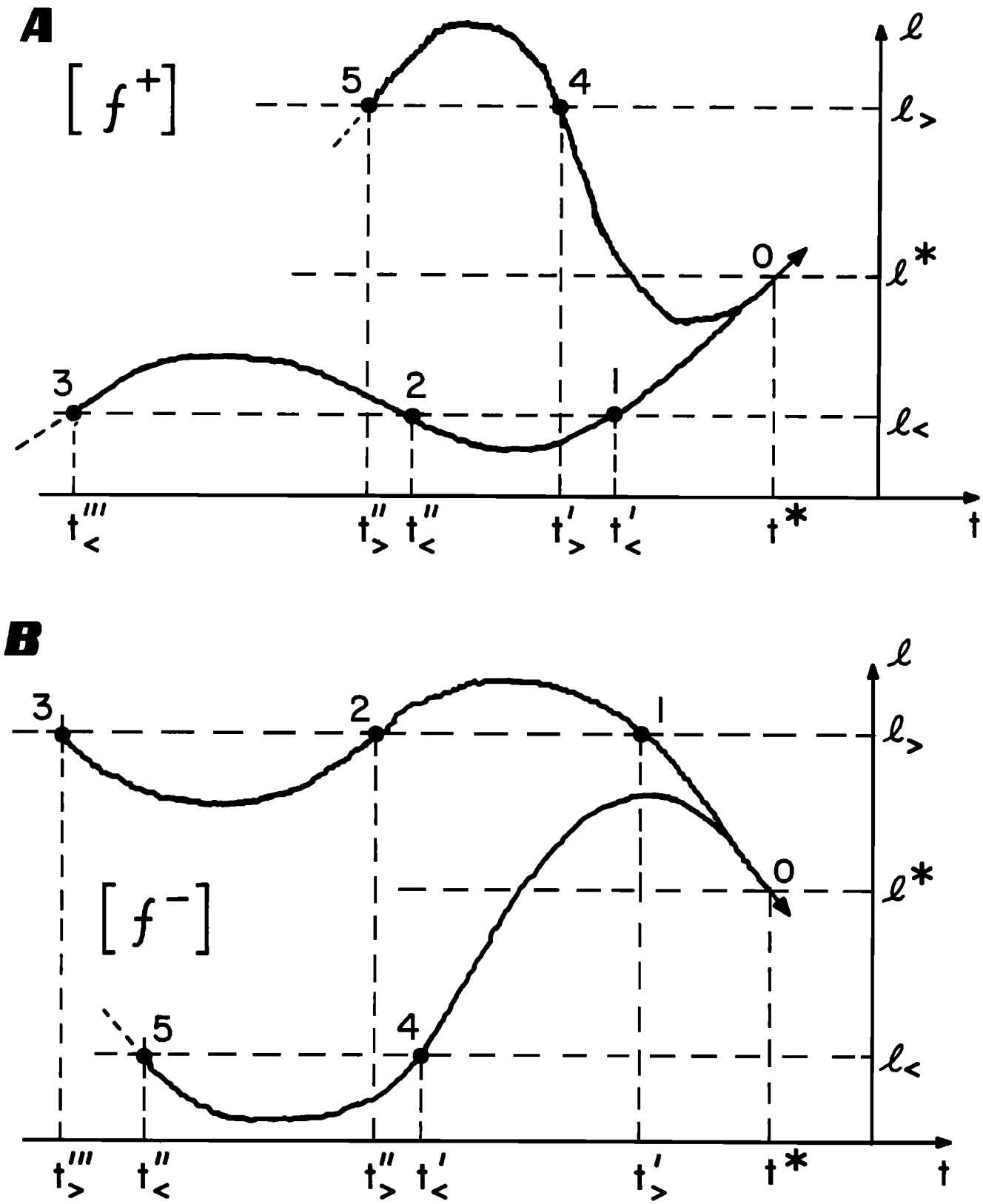

Fig. 2. (*a*) The first five types of space time trajectories with access to (l^*, t^*) with $v^{-*} > 0$. (*b*) The first five types of space time trajectories with access to the same (l^*, t^*) position but with $v = -v^{-*}$. Note that script els of the figure have been typeset in the text as lower case italic els.

We have assumed in deriving (23) that there is sufficient collisional depth (ΔS) outside the observer (for all energies $\gtrsim 1$ keV) that the range of integration to obtain $P^{(1)}$ is practically infinite. We can show that by 10–20 AU in the ecliptic that this is a reasonable assumption. At higher energies the finite size of the heliosphere will make the collision depth outside the observer to the heliopause a finite number which is a decreasing function with energy. This in turn implies that $P^{(1)}$ becomes a decreasing function with increasing energy.

Similarly, the integrated probability $P^{(2)}$ that a particle leaves and returns to the same level after two turning points is

$$P^{(2)} = P^{(1)} \cdot P^{(1)} = (\tfrac{1}{8})^2 \tag{24}$$

since the cumulative survival is a joint probability. By induction, the probability of surviving n turning point trajectories between a source position l' and the same source position at a later time is

$$P^{(n)} = (\tfrac{1}{8})^n \tag{25}$$

Thus the contributions to $\exp(-\Delta S) f_k(\Delta S)$ on the right-hand side of (15) from an 'emission' layer at $l_<'$ for all times t prior to t^*, which is at collisional depth δS to the observer, are

$$\exp(-\Delta S) f_k(\Delta S) = f_k(\delta S[l_<']) \cdot \exp(-\delta S) \cdot \left\{ \sum_{n=0}^{\infty} P^{(n)} \right\}$$

$$+ Q(l_>', l^*) = \tfrac{8}{7} f_k(\delta S[l_<']) \cdot \exp(-\delta S) + Q(l_>', l^*) \tag{26}$$

where $Q(l_>', l^*)$ are the contributions from collisional distributions at $l_>'$ larger than l^*. In deriving (26) we have made use of the fact that the forces considered were conservative, that f_k is isotropic, and that it does not depend explicitly on time.

In Figure 2*a* we also show some of the leading contributions $(4 \to 0)$, $(5 \to 4 \to 0)$ to the additional term Q in (26) which are those contributions to the observed f from the same collisional depth ΔS but source regions beyond that of the observer. In order for these source regions to have access to the same phase space element $d\mathbf{r}^* d\mathbf{v}^*$ about $(\mathbf{r}^*, \mathbf{v}^*)$ as the contributions explicitly given in (26), at least one turning point en route from a collisional distribution to the observer is required. Thus the probability sum for this additional term is exactly that already used minus the first, or direct ascent (descent), term ($P^{(0)} = 1$); therefore the complete expression for (26) for all contributions from arc lengths $l_<$, $l_>$ such that $\exp(-\delta S)$ is the no-scattering probability to survive from $l_< \to l_*$ or $l_> \to l_*$, for particles with a specific positive $dl/dt = v_\parallel$, and energy E at (l^*, t^*) is

$$\exp(-\Delta S) f_k(\Delta S)|^+ = \exp(-\delta S)$$

$$\cdot \{\tfrac{8}{7} f_k(l_<[\delta S]) + \tfrac{1}{7} f_k(l_>[\delta S])\} \tag{27}$$

For particles at l^* moving toward the sun (i.e., negative cosines of their pitch angle) (Figure 2*b*), direct access to the phase space element $(\mathbf{r}^*, \mathbf{v}^*)$ is not possible from inside; rather, only from outside; reversing the weighting of (27), we obtain

$$\exp(-\Delta S) f_k(\Delta S)|^-$$

$$= \exp(-\delta S)\{\tfrac{1}{7} f_k(l_<[\Delta S]) + \tfrac{8}{7} f_k(l_>[\delta S])\} \tag{28}$$

When (27) and (28) are normalized by the condition

$$\lim_{\Delta S \to 0} \exp(-\Delta S) f_k(\Delta S)|^{\pm} = f_k(\Delta S = 0) \tag{29}$$

(27) and (28) become

$$\exp(-\Delta S) f_k(\Delta S)|^+$$

$$= \exp(-\delta S)\{\tfrac{8}{7} f_k(l_<[\delta S]) + \tfrac{1}{7} f_k(l_>[\delta S])\} \tag{30}$$

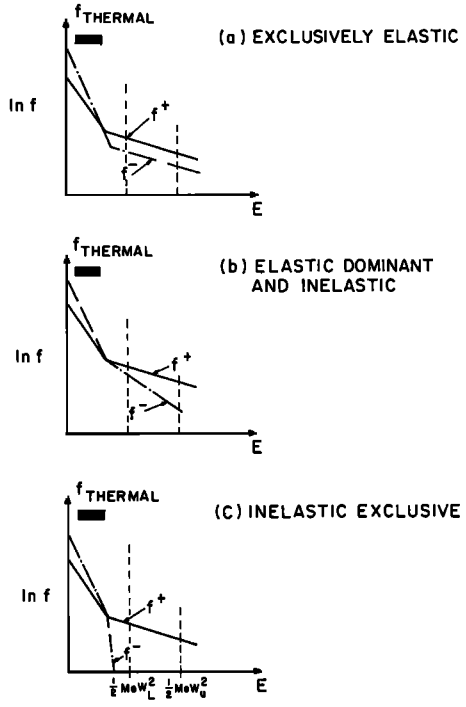

Fig. 3. Schematic of fore (f^+) and aft (f^-) electron distribution functions under different assumptions of the dominant manner in which suprathermals are backscattered. A Maxwellian in this format is a straight line. (*a*) Exclusively elastic: in this limit $f^+/f^- \to \infty$ for $E > 7kT_c$ and $-dE/d \ln f^+ = -dE/d \ln f^-$ in extrathermal regime. (*b*) Elastic dominant plus inelastic: $(-dE/d \ln f^+) > -(dE/d \ln f^-)$ for extrathermals; $(-dE/d \ln f^-)_{\text{extra}} > (-dE/d \ln f)_{\text{thermal}}$. (*c*) Inelastic exclusive: $(-dE/d \ln f^+) > (-dE/d \ln f^-)_{\text{extra}}$, but $(-dE/d \ln f)_{\text{extra}} < (-dE/d \ln f)_{\text{thermal}}$; $(-dE/d \ln f^-)_{\text{extra}} \sim k_B T(R^*)$, where R^* is the distant radial position where extrathermals have lost so much kinetic energy as to become a member of the local Maxwellian with $T(R^*)$.

and

$$\exp(-\Delta S) f_k(\Delta S)|^-$$

$$= \exp(-\delta S)\{\tfrac{1}{7} f_k(l_<[\delta S]) + \tfrac{8}{7} f_k(l_>[\delta S])\} \tag{31}$$

Equation (15) then becomes explicitly

$$f^+\{t[l^*(r)]\} = \left\{\left(\frac{6}{7}\right) f_k[t_0(r_L)] + \left(\frac{1}{7}\right) f_k[t_0(r_u)]\right\} \exp(-S_0)$$

$$+ \left(\frac{6}{7}\right) \int_{r_L(t_0)}^{r[l^*(t)]} \exp(-\delta S[t'(r')]) \frac{f_k[t'(l'(r'))]}{\tau[t'(l'(r'))]} \frac{dt'}{dl'} \frac{dl'}{dr'} dr'$$

$$+ \left(\frac{1}{7}\right) \int_{r_U(t_0)}^{r[l^*(t)]} \exp(-\delta S[t'(r')]) \frac{f_k[t'(l'(r'))]}{\tau[t'(l'(r'))]}$$

$$\cdot \frac{dt'}{dl'} \cdot \frac{dl'}{dr'} \cdot dr' \tag{32a}$$

$$f^-\{t[l^*(r)]\} = \left\{\left(\frac{1}{7}\right) f_k[t_0(r_L)] + \left(\frac{6}{7}\right) f_k[t_0(r_u)]\right\} \exp(-S_0)$$

$$+ \left(\frac{1}{7}\right) \int_{r_L(t_0)}^{r[l^*(t)]} \exp(-\delta S[t'(r')]) \frac{f_k[t'(l'(r'))]}{\tau[t'(l'(r'))]} \frac{dt'}{dl'} \frac{dl'}{dr'} dr'$$

$$+ \left(\frac{6}{7}\right) \int_{r_U(t_0)}^{r[l^*(t)]} \exp(-\delta S[t'(r')]) \frac{f_k[t'(l'(r'))]}{\tau[t'(l'(r'))]}$$

$$\cdot \frac{dt'}{dl'} \cdot \frac{dl'}{dr'} \cdot dr' \tag{32b}$$

where r_L, r_U are given below in (35*d*), (35*e*).

From the Parker topology of the interplanetary field defined by bulk speed U, solar rotation rate Ω, at location r' and ecliptic colatitude θ', we have

$$\frac{dl'}{dr'} = \frac{[(r'\Omega \sin\theta')^2 + U^2]^{1/2}}{U} \tag{33}$$

We note that $r(l^*) \leq r_u(t_0)$, that

$$\left(\frac{dt'}{dl'}\right)^{-1} = \frac{dl'}{dt'} = + \left|\frac{dl'}{dt'}\right|$$

in the first integral of (32*a*) and (32*b*), that

$$\frac{dl'}{dt'} = - \left|\frac{dl'}{dt'}\right|$$

in the second integral of (32*a*) and (32*b*), and that

$$\left|\frac{dl'}{dr'}\right| = |v_{\|}(r')| \neq 0$$

By conservation of energy and magnetic moment we have

$$\frac{1}{2}m_e v_{\|}^2(r') = \frac{1}{2}m_e v_{\|}^2(r) + \frac{1}{2}mv_{\perp}^2(r)\left[1 - \frac{B'}{B}\right] - [e\phi(r) - e\phi(r')] \tag{34}$$

where $\phi(r)$ is the interplanetary electrostatic potential and $m_e v_{\|}$ and $m_e v_{\perp}$ are the particle's components of momentum along and transverse to B. The gravitational terms in the conservation of energy have been neglected.

Thus (32*a*), (32*b*) may be computed as integrals over ordinary space to be

$$f^+\{t[l^*(r)]\} = \left\{\left(\frac{6}{7}\right)f_k[t_0(r_L)] + \left(\frac{1}{7}\right)f_k[t_0(r_U)]\right\}\exp(-S_0) + \left(\frac{6}{7}\right)\int_{r_L(t_0)}^{r[l^*(t)]} \exp(-\delta S)\frac{f_k[t'(r')]}{\tau[t'(r')]} \cdot \frac{[(r'\Omega\sin\theta')^2 + U^2]^{1/2}}{U}\frac{dr'}{v_{\|}[t'(r')]} + \left(\frac{1}{7}\right)\int_{r[l^*(t_0)]}^{r_U(t_0)} \exp(-\delta S)\frac{f_k[t'(r')]}{\tau[t'(r')]} \cdot \frac{[(r'\Omega\sin\theta')^2 + U^2]^{1/2}}{U}\frac{dr'}{v_{\|}[t'(r')]} \tag{35a}$$

$$f^-\{t[l^*(r)]\} = \left\{\left(\frac{1}{7}\right)f_k[t_0(r_L)] + \left(\frac{6}{7}\right)f_k[t_0(r_U)]\right\}\exp(-S_0) + \left(\frac{1}{7}\right)\int_{r_L(t_0)}^{r[l^*(t)]} \exp(-\delta S)\frac{f_k[t'(r')]}{\tau[t'(r')]} \cdot \frac{[(r'\Omega\sin\theta')^2 + U^2]^{1/2}}{U}\frac{dr'}{v_{\|}[t'(r')]} + \left(\frac{6}{7}\right)\int_{r[l^*(t_0)]}^{r_U(t_0)} \exp(-\delta S)\frac{f_k[t'(r')]}{\tau[t'(r')]} \cdot \frac{(r'\Omega\sin\theta')^2 + U^2]^{1/2}}{U}\frac{dr'}{v_{\|}[t'(r')]} \tag{35b}$$

The most prominent advantage of (35*a*) and (35*b*) is that all explicit references to turning point orbits are absorbed into the coefficients of 1/7 and 6/7. The remaining quadratures are for unscattered orbits between collisional depth δS and the observer. It is this circumstance which allows the use of collisionless guiding center relationships, (34), to determine the spatial matchups of a particle with collisional depth δS between ($\mathbf{r}^*$, $\mathbf{v}^*$) and ($\mathbf{r}'$, $\mathbf{v}'$).

The limits of integration in (32*a*), (32*b*) and (35*a*), (35*b*) are determined in the following way. The phase space map for an unscattered particle between 'sources' $r_>$, $r_<$ and observer is given by (1) the pitch angle map,

$$\cos[\theta(r_{\gtrless})] = \mp[1 - \mu^* B(r_{\gtrless})/mv^2(r_{\gtrless})]^{1/2} \tag{35c}$$

and (2) energy conservation,

$$\tfrac{1}{2}m_e v^2(r_{\gtrless}) + Z_- e\phi(r_{\gtrless}) = \tfrac{1}{2}m_e v^2(r^*) + Z_- e\phi(r^*)$$

where $\mu^* = mv_{\perp}^2(r_*)/B(r_*)$, $Z_- = -1$, and $r_{\lessgtr}$ refer to source regions outside ($r_>$) or inside ($r_<$) that of the observer.

Since cos θ must be real, the pitch angle map places spatial bounds on the integrals considered:

$$0 \leq \frac{mv^2(r_{\gtrless})}{B(r_{\gtrless})} \leq \mu^*$$

thus implicitly defining r_U, r_L

$$\frac{mv^2(r_{UL})}{B(r_{U,L})} \equiv \mu^*$$

If $|\mathbf{B}(r)|$ and ϕ are monotonic functions, there are only two roots. Energy conservation also places a constraint on the radial domain of integration:

$$0 \leq \tfrac{1}{2}mv^2(r_{\gtrless}) = \tfrac{1}{2}mv^2(r^*) + Z_- e\phi(r^*) - Z_- e\phi(r_{\gtrless})$$

In practice this last constraint only impacts r_U because the particle is giving up kinetic energy as r increases.

For the special case of $\mu^* = 0$ the radial limits of integration are determined implicitly by

$$\tfrac{1}{2}mv^2(r_U) = \tfrac{1}{2}mv^2(r^*) + Z_- e\phi(r^*) - Z_- e\phi(r_U) \tag{35d}$$

and r_L is the smallest radius for which $f_k(r_L)$ has sufficient population at kinetic energy

$$\tfrac{1}{2}mv^2(r_L) = \tfrac{1}{2}mv^2(r^*) + Z_-[e\phi(r^*)] - Z_-[e\phi(r_L)] \tag{35e}$$

to be detected in comparison with the local distribution. For all the 'realizations' which we discuss, $\mu^* = 0$ and $r_L = 1.03\,R_S$.

The elastic scattering approximation used to obtain (35*a*) and (35*b*) is most accurate for extrathermal electrons and will be relaxed in paper 4. The principal impact of this approximation is to limit the precision of the predictions of the sunward propagating extrathermal phase density in the transthermal and extrathermal regime. The predictions of the current formulation for the outward propagating extrathermal population are essentially independent of this assumption.

If only elastic scattering is considered, then, as shown schematically in Figure 3*a*,

$$\lim_{w\to\infty}\frac{f^-(\frac{1}{2}mw_{\|}^2)}{f^+(\frac{1}{2}mw_{\|}^2)} = \frac{1}{6}$$

independent of energy in the extreme extrathermal regime. The superscripts on f denote cuts of distribution function along (plus) and, opposed (minus) to the outward ray along the tubes of force. In support of our theoretical arguments that elastic collisions should be more important than inelastic in determining $f^-(\frac{1}{2}mw^2)$, we discuss an experimental determination of f^-/f^+ as a function of energy in Figure 4. Here we have plotted the ratio,

$$R = f^-(w_{\|})/f^+(w_{\|})$$

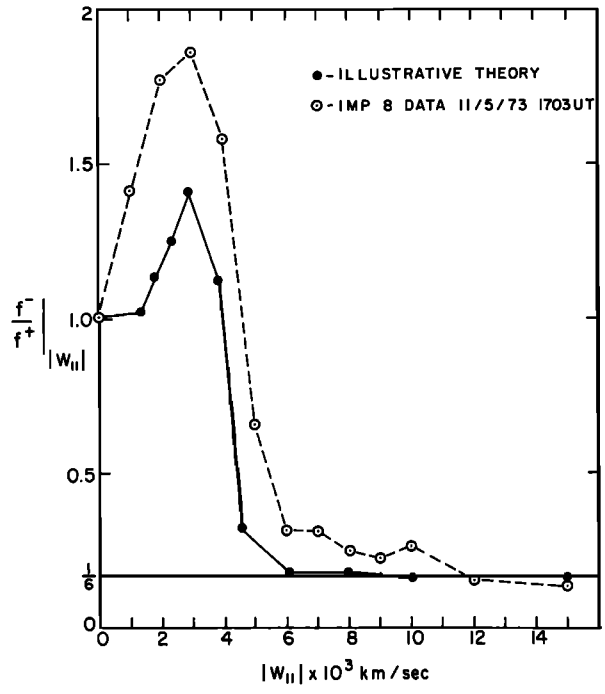

Fig. 4. The ratio of fore to aft phase density (f^+/f^-) as a function of proper frame velocity parallel to B, as adapted from published data (open circles, *Feldman et al.* [1975]); solid dots from illustrative theory (this paper, Figure 8). Horizontal line gives theoretical asymptote of $\frac{1}{6}$ which prevails for the excusively elastic case of Figure 3*a*.

versus parallel proper frame speed $|w_\parallel|$ for a published example of Imp 8 data (open circles). We have indicated the theoretical asymptote of $\frac{1}{6}$ which follows from ignoring inelastic collisions. The experimental data for this published example do asymptote in the vicinity of the theoretical value of $\frac{1}{6}$. (The solid circles show the trends of a 'realization' discussed in section 6.)

If inelastic Coulomb scattering assists extrathermal backscattering via the speed dependence of the cross section, then

$$\frac{f^-(\frac{1}{2}mw_L^2)}{f^-(\frac{1}{2}mw_U^2)} > \frac{f^+(\frac{1}{2}mw_L^2)}{f^+(\frac{1}{2}mw_U^2)} \qquad 2w_{T,e} \lesssim w_L < w_U$$

where the subscripts refer to lower and upper proper frame speeds in the sense of the above inequality. Acceptable w_L and w_U are indicated in Figure 3. This relation implies that the differential slope of the extrathermal population going toward the sun will determine a cooler differential temperature than that going away (Figures 3*b* and 3*c*) if Coulomb collisional losses are a substantial factor in the extrathermal backscattering history. In the extreme limit of completely inelastic backscattering the extrathermal temperature of f^- may even be cooler than that of the local thermal population (Figure 3*c*).

The exclusive elastic case of Figure 3*a* is the most conducive to fitting the halo subpopulation with a drifting bi-Maxwellian, where by construction

$$-\frac{dE}{d\ln f^+} = -\frac{dE}{d\ln f^-}$$

(extrathermal regime), as is implicit in the modeling done by *Feldman et al.* [1975] for a wide variety of data. Nevertheless, the average normalized χ^2 for these parameterizations is rather high, indicating a probable admixture of some inelastic backscattering (Figure 3*b*). In this latter circumstance the least squares model of a drifting bi-Maxwellian is no longer sufficiently flexible to accommodate this spectral shape. If a bi-Maxwellian is forced to fit data as schematized in Figure 3*b*, it will result in a larger normalized χ^2 than data as schematized in Figure 3*a*.

5. Implementation

In order to carry out the integrals indicated in (35*a*) and (35*b*) we need to specify the profiles of the electron and proton temperatures, their density, and the gravitational, electric, and magnetic fields. The first three requirements define the Krook approximation to the collision operator through (7) by determining $f_k^{(0)}(\mathbf{r})$ and $\tau[f_k^{(0)}(r)]$; the last three profiles define the force field $\mathbf{F}$ of the Boltzmann evolution operator (1).

In Figure 5 we show a density profile, developed by *Sittler and Olbert* [1977] and *Sittler* [1978] from composite experimental sources, which we will adopt to be the density for $f_k^{(0)}$. In Figure 6 we show the empirical estimates of the radial variations of $T_{\text{thermal}}{}^{\text{electron}}$. Near the sun we have used the measurements and arguments of *Bame et al.* [1974], who suggest that $T_e \propto r^{-2/7}$ near the base of the corona. We have used the results of *Ogilvie and Scudder* [1978] using data between 0.45 and 0.85 AU that T_e, thermal, varies like $r^{-0.8}$ and the results of K. I. Gringauz and M. I. Verigin (unpublished manuscript, 1975) for $1 < r < 1.5$ AU and an asymptotic adiabatic behavior at large distances (>10 AU). We have constrained the electron profile to agree with 1.5×10^5 °K at 1 AU and to be 1.0×10^6 °K near 1 R_S, consistent with coronal hole temperature estimates given by *Maxson and Vaiana* [1977].

To evaluate the Coulomb logarithm and assess overall energetics, a proton thermal profile is also required. We assume $T_e(r) = T_p(r)$ for all radii inside that radial distance $r = R$ beyond which adiabatic cooling determines the average $\langle T_p(1\text{ AU})\rangle \sim 7 \times 10^4$ °K. R is usually 60–90 R_S, consistent, for

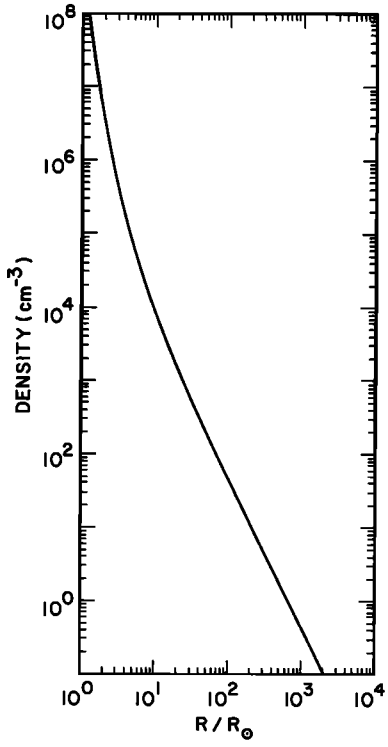

Fig. 5. Radial density profile after *Sittler and Olbert* [1977] and *Sittler* [1978].

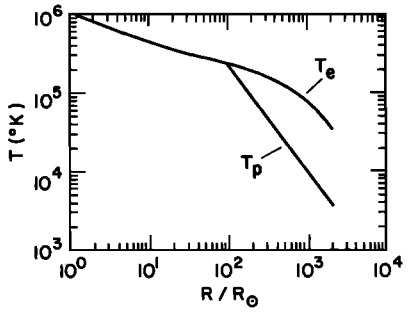

Fig. 6. Radial thermal electron and proton temperature profile. Constructed as described in text based on empirical constraints.

example, with the two fluid results of *Acuña and Whang* [1976]. The solutions and the energetics are relatively insensitive to the large r radial dependence of T_p because the thermal forces on the flow are so small.

We have used the generalized Ohm's Law (cf., e.g., *Rossi and Olbert* [1970], p. 350, equation (12.26)) to self-consistently estimate the time average parallel electric field in the proper frame of the plasma, $E_\parallel{}^*$:

$$(E_\parallel{}^*)_T \equiv (\mathbf{E}\cdot\langle\hat{\mathbf{B}}\rangle)_T = \left(\frac{-\nabla\cdot \mathsf{P}_e}{en_e}\cdot\langle\hat{\mathbf{B}}\rangle\right)_T + (E_\parallel{}')_T \qquad (36)$$

where the additional effective electric field $E_\parallel{}'$ is given by

$$(E_\parallel{}')_T = \frac{m_e}{n_e e^2}\left(\left[\frac{e}{m_e}(\mathbf{j}^*\times\mathbf{B}) + \frac{d\mathbf{j}^*}{dt} + (\mathbf{j}^*\cdot\nabla)\mathbf{U} + \mathbf{j}^*(\nabla\cdot\mathbf{U}) + (\mathbf{U}\cdot\nabla)\mathbf{j}^* + \eta\left(\frac{d\mathbf{U}}{dt} - \mathbf{g}\right) - \frac{\delta\mathbf{j}^*}{\delta t}\bigg|_{\text{collisions}}\right]\cdot\langle\hat{\mathbf{B}}\rangle\right)_T$$

where η is the fractional net charge density, the angular brackets denote a spatial average, and the parentheses $(\ )_T$ denote a temporal average over a multiple of fluctuating cycles.

The last term in (36) is nonzero when there are currents in the proper frame, waves propagating in the system, or deviations from charge neutrality. In most circumstances the Hall effect term (the first one in $E_\parallel{}'$) is the most important. It can be shown that Alfvénic fluctuations, for example, give a nonzero contribution to $(E_\parallel{}')_T$. Generically, $(E_\parallel{}')_T$ represents the consequences of uncompensated forces in the proper frame of the plasma which have a nonvanishing time-averaged component along $\langle\hat{\mathbf{B}}\rangle$.

Given the current state of our understanding of waves and their time-averaged current systems $\mathbf{j}^*$ in the solar cavity, it is difficult to estimate $E_\parallel{}'(r)$ with precision. Nevertheless, the order of magnitude of the potential energy barrier which this additional electric field produces is of the order of the wave work necessary to have an energetically self-consistent solar wind expansion:

$$\text{work}|_{\text{wave}} = \frac{1}{2}(m_e + m_p)U_\infty{}^2 + GM_S(m_e + m_p)/1.03\,R_S + \int_{1.03R_S}^{\infty}\frac{\nabla\cdot \mathsf{P}_e + \nabla\cdot \mathsf{P}_t}{n(r')}\cdot d\mathbf{r}' \qquad (37)$$

To be effective in accelerating the solar wind to the observed speeds, this wave work is expected to be done within the sub/trans Alfvénic region of the solar wind expansion [*Belcher*, 1971]. We introduce a scale, L_{wave}, over which this work is principally done and phenomenologically have incorporated the potential barrier due to $E_\parallel{}'(r)$ as

$$Z_- e[\phi(R) - \phi(1.03\,R_S)] = \int_{1.03R_S}^{R} e\mathbf{E}^*\cdot d\mathbf{s} = A\tanh\left(\frac{r - 1.03\,R_S}{L_{\text{wave}}}\right) \qquad (38)$$

where $A \sim \text{work}|_{\text{wave}}$ from energy conservation considerations. This portion of the total electrostatic barrier for electrons achieves 76% of its asymptotic value at $r_{76\%} = 3L_{\text{wave}} + 1.03\,R_S$. Our assumption of the form of the additional electrostatic barrier (38) corresponds to an effective electric field which is strongest near the base of the corona and goes to zero as e^{-Z^2}, $Z = (r - 1.03\,R_S)/L_{\text{wave}}$.

We have therefore used an electrostatic parallel electric field of the form

$$E_\parallel{}^* = -\frac{(\nabla\cdot \mathsf{P}_e)\cdot\langle\hat{\mathbf{B}}\rangle}{en_e} + \frac{A}{eL_{\text{wave}}}\,\text{sech}^2\left(\frac{r - 1.03\,R_S}{L_{\text{wave}}}\right) \qquad (39)$$

for a positive magnetic sector.

When solutions are reported below, L_{wave} will be a parameter, but usually of the order of $5\,R_S$. With these considerations the interplanetary potential is energetically self-consistent with the asymptotic wind speed used to define the topology of the magnetic lines of force.

In Figure 7 we show the interplanetary potential which results from integrating $E_\parallel{}^*$ along a typical field line with Parker topology when the above empirical profiles of $n_e(r)$, $T_e(r)$, and $E_\parallel{}'(r)$ are used. The asymptotic flow speed was assumed for this example to be 400 km/s, and L_{wave} was $5\,R_S$. Shown for comparison is an interplanetary potential profile reported by *Lemaire and Scherer* [1973] using an exospheric solar wind model.

This electrical potential represents a significant barrier for the escape of electrons from the proximity of the lower corona; at the same time it is an acceleration for the positive ions. An electric field of this type is implicit in fluid solar wind models which externally impose the local condition that the bulk speeds and densities of the electrons and ions be equal (cf., e.g., *Hartle and Sturrock* [1968]). This type electric field is also implicit (through the assumption $j^* = 0$) in the *Spitzer and Härm* [1953] collision-dominated coefficient of thermal conduction which is often used in solar wind models. The electric field used in this reference is predicated on local thermodynamic equilibrium (LTE), which is not justified in the solar wind.

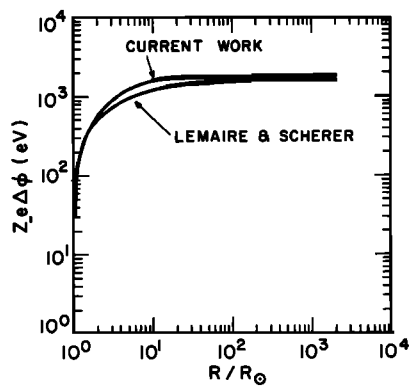

Fig. 7. Self-consistent change in potential energy for an electron where the zero of potential has been shifted to the base of the corona. An electron gives up kinetic energy which is stored as this potential change in leaving the lower corona.

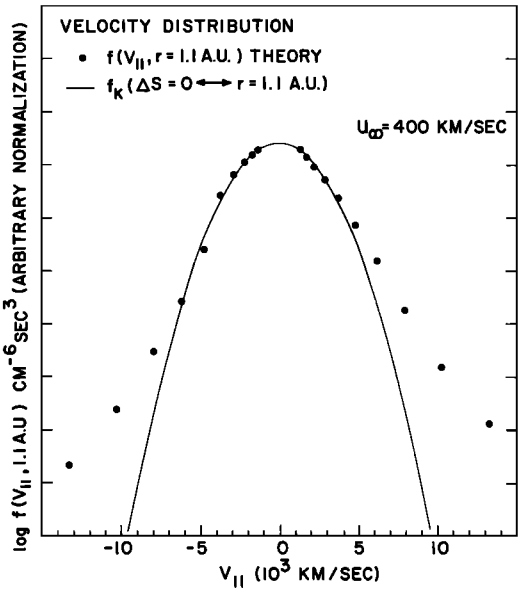

Fig. 8. Theoretical profile of $f^{(1)}(v_\parallel{}^*, R^* \sim 1.1$ AU) for U_∞ = 400km (solid circles); $f_k{}^{(0)}(\Delta S = 0)$ used in solution (solid curve); see text for details.

6. Results

The results of two realizations of the formal solution (15) will now be discussed in some detail. The two realizations differ by the asymptotic flow speed attained by the solar wind but refer to the same spatial location of 1.1 AU.

General Features of Solutions

The solid circles in Figure 8 show a cut of the electron distribution function along the local magnetic field line at time t and position r = 1.1 AU, as a result of the numerical integration of (15)–(35*b*) considering only Coulomb collisions. The asymptotic wind speed was 400 km/s, and L_{wave} was taken to be 5 R_S. The solid curve is the local assumed form of $f_k{}^{(0)}(\Delta S = 0, V_\parallel)$, which is given for reference. Comparing the computed distribution (solid circles) with the solid curve and referring to (16) or (17), we see that the differences between the two curves are due to the integrated contributions originating away from the observer.

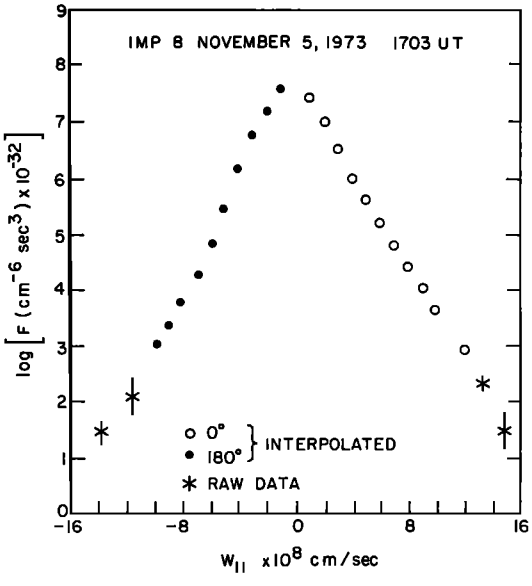

Fig. 9. Observed $f(v_\parallel, r \sim 1$ AU) adapted (unfolded) from *Feldman et al.* [1975], Figure 1.

In Figure 9 are shown fore and aft cuts along the local magnetic field of f_e near 1 AU reported by *Feldman et al.* [1975]. The data of their Figure 14 have been transformed into the proper frame using the bulk velocity given in Figure 3 of that paper, which was 520 km/s. Although we have not tried to fit the observed profiles by adjusting various parameters, we find there is a remarkable similarity between the theoretical profile Figure 8 and the data Figure 9. We draw particular attention to the correspondences in (1) size, (2) shapes, and (3) skewness between the theoretical and experimental profiles. Of course, this is not a complete comparison which would require a theoretical determination of the entire pitch angle distribution.

It is instructive to characterize the location where the thermal and extrathermal populations at 1 AU were last members of the thermal collisional population. In order to do this we recast the integrals of (35*a*) and (35*b*) as

$$f^+ = \left(\frac{6}{7}\right) \sum_i \Delta f(\vec{R}_i', R, l' < l^*) + \left(\frac{1}{7}\right) \sum_j \Delta f(\vec{R}_j', R, l' > l^*) \quad (40a)$$

$$f^- = \left(\frac{1}{7}\right) \sum_i \Delta f(\vec{R}_i', R, l' < l^*) + \left(\frac{6}{7}\right) \sum_j \Delta f(\vec{R}_j', R, l' > l^*) \quad (40b)$$

where $\Delta f(\vec{R}_i, R)$ is the integral over the integrands of (35*a*), (35*b*) but with limits of $\vec{R}_i' \pm \Delta R_i$ such that

$$\vec{R}_i' + \Delta R_i = \vec{R}_{i+1}' - \Delta R_{i+1} \quad (41)$$

In Figure 10 we have indicated the spatial location of the collisional distributions which dominate the populations of two energy extremes of the theoretical profile given in Figure 8. The value of the theoretical profile at the given energy in Figure 8 is the corresponding area under the indicated curves in Figure 10.

Figure 10 clearly restates the local character of the thermal population. The dominant contributions for particles of 5-eV kinetic energy near earth come from within ±0.2 AU (less than the thermal mean free path) of the observer. The forward pitch angle population at 5 eV (θ = 0) comes predominantly from collisional populations sunward of the observer; for θ = 180° at 5 eV the converse is true, as shown in the shaded contribution.

In the extrathermal regime (as an extreme example, kinetic energy 500 eV) we see that both forward (θ = 0) and aft (θ = 180°) populations were last members of a collisional distribution deep in the base of the corona (<3 R_S) and certainly near the site of the initial expansion of the solar wind. This is the same area where theoretical extrapolation of Mariner 10 radial variations of $T_c(r)$ and $T_h(r)$ predicted a single Maxwellian distribution. The particles observed at 500 eV propagating toward the sun at 1 AU (θ = 180°) are the backscattered fraction of the outward propagating 500-eV particles which passed the radial distance of the observer at some earlier time prior to their detection. The contributions to Δf^+ and Δf^- (500 eV) are essentially in the ratio of 6:1.

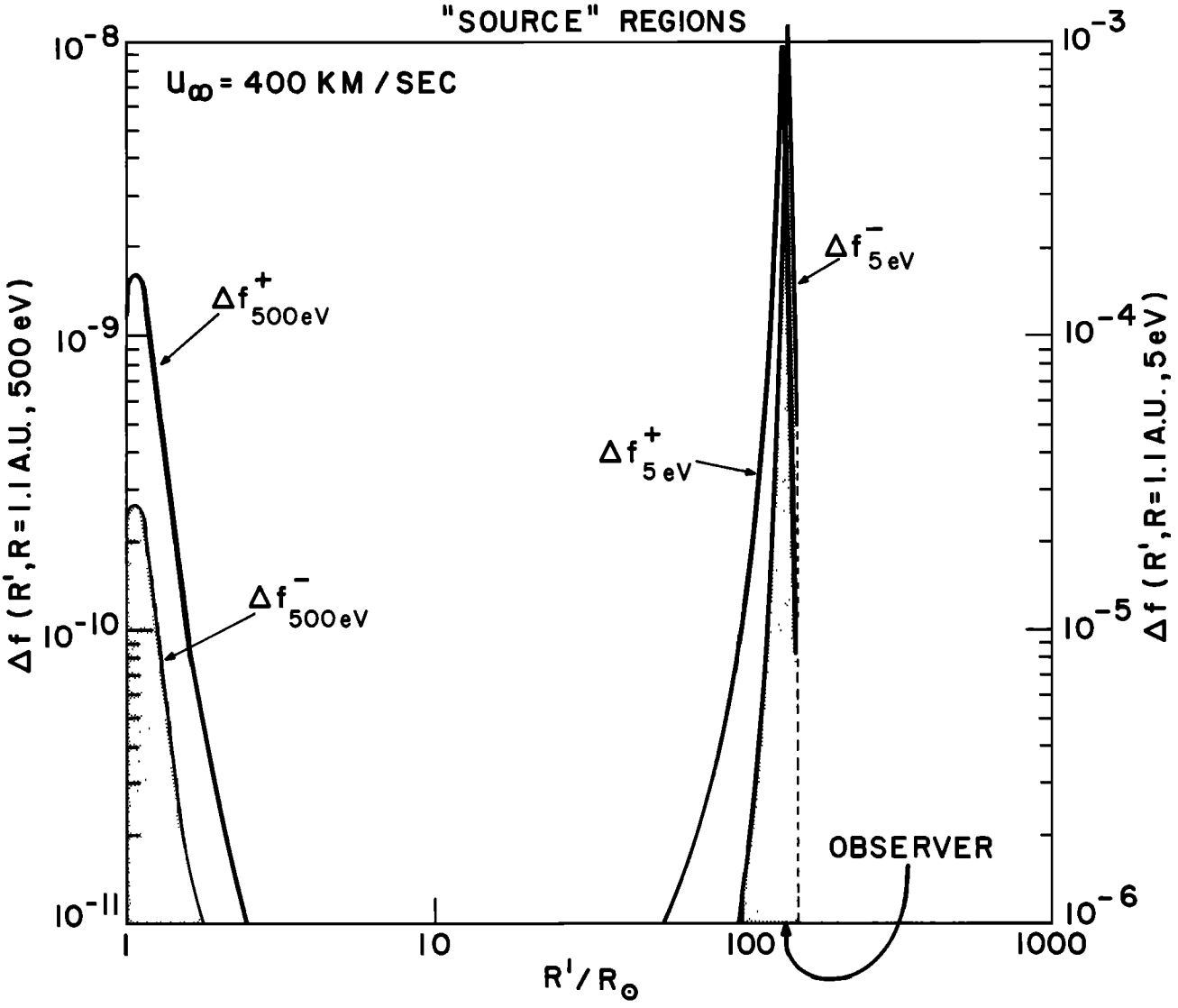

Fig. 10. Spatial locations (R') of the dominant contributions $\Delta f(R', R^*, v_\parallel{}^*, E^*)$ which determine $f^{(1)}(v_\parallel{}^*, R^*)$ in Figure 8. The low-energy (5 eV) thermal population were last members of a collisional distribution very near the observer. The high-energy (500 eV at 1 AU) extrathermals (halo) $\theta = 0$ and $\theta = 180°$ were last members of a collisional distribution deep in the corona. The $\theta = 180°$ halo particles are scattered backward toward the observer at $R' \sim 2$–10 AU, which is outside the observer's position of ~1.1 AU.

The particles with kinetic energies intermediate between these two extremes have collisional antecedents which vary continuously between the two extremes depicted in Figure 10. For some intermediate locally transthermal energies there are two domains of equal importance (i.e., $\Delta f(R', R)$ is two humped). For locally subthermal energies ($E < kT_c$) the smaller contribution is at the sun. As the local energy becomes increasingly extrathermal, the dominant collisional antecedent of the observed $f_e^\pm$ recedes to lower and lower levels in the corona.

The reason for these distributed contributions to the locally observed f_e is intimately related to the spatial variation of the interplanetary potential and the variation with energy of the Coulomb collisional depth of the observer from the sun.

An observed electron of kinetic energy $\frac{1}{2}mv^2(R)$ is energetically accessible from a level R' provided the kinetic energy at R' is

$$\tfrac{1}{2}m_e v^2(R') = \tfrac{1}{2}mv^2(R) + Z_- e[\phi(R) - \phi(R')] \quad (42)$$

These accessible orbits make an observable contribution to the electron distribution function at R provided that a sufficient fraction can survive collisional extinction en route from $R' \rightarrow R$, as compared with the local collisional Maxwellian:

$$f_k[R', \tfrac{1}{2}m_e v^2(R')] \cdot \exp\{-\delta S[R', R, \tfrac{1}{2}m_e v^2(R)]\} \gtrsim f_k[R, \tfrac{1}{2}mv^2(R)] \quad (43)$$

From Figure 7 we see that $Z_-[e\phi(R) - e\phi(R')]$ is positive (negative) for $R' < R$ ($R' > R$). Thus the electrons detected near earth have given up nearly 1 keV of kinetic energy en route from the corona to the observer. Electrons with energy of 500 eV at 1 AU had a kinetic energy of ~1.5 keV in the coronal Maxwellian population of characteristic energy of ~ 100 eV, 15 standard deviations off of the maximum phase density at $R' \sim 1$–2 R_S. Because the relative density of the lower corona becomes large so rapidly and because $\delta S(R', R,$ 500 eV) is so small, $\Delta f(R', R)$ can give a measurable phase density signal to the observer near 1 AU.

On the other hand, because the Coulomb collisional extinction δS depends so strongly on the kinetic energy of the particle (cf. (13) and (17)), it is very difficult to get nonlocal contributions to f observed for subthermal energies ($E < kT_c(R)$). Although condition (42) is readily met at a reasonable range of nonlocal R's, the survival probabilities are so small ($\delta S(R', R)$ for kinetic $E < k_BT$ are so large) that only those collisional distributions within the vicinity can survive to the observer. (Mathematically, $\delta S(R', R) \to 0$ for any E provided $R'(t') \to R(t)$ is small enough: cf. (12).)

We thus see that the population of the forward extrathermals should in steady state be a very sensitive indicator of the interplanetary potential barrier between the base of the corona and the observer. The best local indicator of a large potential barrier to the corona for electrons is a higher solar wind speed, other things being equal such as the $(\nabla \cdot P_e)/n(r)$ contribution to the potential drop.

The above conclusion implies an anticorrelation between local plasma bulk speed (if it is nearly the asymptotic bulk speed) and the local fractional extrathermal (n_{halo}/n) phase density. From our discussion of Figure 10 we should not interpret this as a local cause and effect relationship; rather, the cause of both local effects is in the strong acceleration region removed by 1 AU from the observer. This global sense of causality in the inner heliosphere must prompt reexamination of the use of transport coefficients and equations of state which by definition relate local forces to local responses. We return to these matters in detail in paper 3.

In Figure 11 we show in the same format as in Figure 8 a solution for U_∞ = 800 km/s with L_{wave} still equal to 5 R_S and all other parameters that are independently specifiable the same. As was explained previously, the net wave work is adjusted to give consistency to the expansion energetics and magnetic topology. As can be readily seen, the suprathermal population is depleted in a relative sense as we qualitatively expected. Furthermore, the estimate of the 'differential temperature' for the suprathermals is also reduced when the asymptotic flow speed is increased. The heat flux $|q_e|$ depends on the number of carriers available, and it is known that the most important contribution to $|q_e|$ at 1 AU occurs between 25 eV and 130 eV [*Scudder*, 1970; *Montgomery*, 1970] centered on the break region. If we thus deplete this population and lower its most probable speed ($\alpha T_{eff}^{1/2}$), the heat flux it carries must also be reduced. We thus expect on the basis of this model that the interplanetary heat flux density in quasi-steady-state flows should be anticorrelated with the local bulk speed. As before, this is a global cause with two local signatures: $|U|$ and $|q_e|$. There is thus no intrinsic local thermodynamic interrelationship between $|q_e|$ and $|U|$; rather, there is a global integro-differential interrelationship between the whole expansion history of the flow tube and all pressure and density gradients (which determine $E_\parallel$) along it.

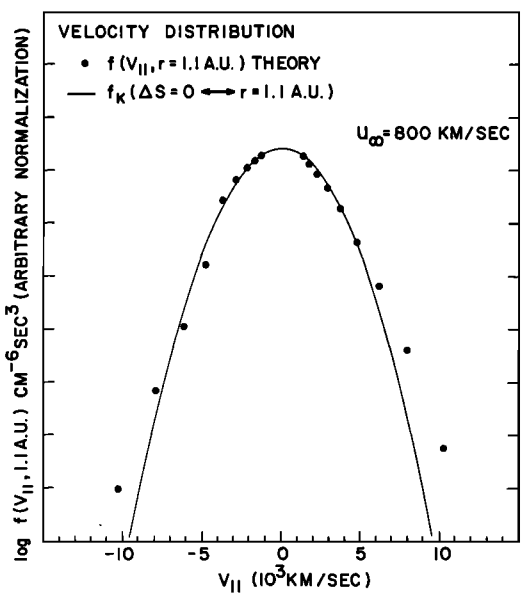

Fig. 11. Theoretical profile of $f^{(1)}$ ($v_\parallel$*, $R^* \simeq 1.1$ AU) for U_∞ = 800 km/s (solid circles). Solid curve is $f_k^{(0)}(v_\parallel, \Delta S = 0)$: see text.

Figure 12 shows the dominant spatial contributions to the 5- and 500-eV points of Figure 11. Note the changed scale of the left ordinate relative to Figure 10. In this higher-speed (U_∞ = 800 km/s) example, the deep corona is essentially inaccessible to the normal halo population. The sparser contributions come from 8–20 R_S, with somewhat cooler collisional populations which are sufficiently populated at the correct shifted energies to have energetic access and phase density excess sufficient to overcome extinction. The contributions to the local population of f remain essentially immune to the change in the global dynamics, which in this example merely changes the floating potential of the vicinity of the observer by a constant amount.

Thermal Domain Effects of Scattering

Returning to Figures 8 and 11 and concentrating on the subtransthermal portion of the distribution, we see on first impression that the results of the scattering have not changed the local distribution. However, the slight departures of the dots from solid $\Delta S = 0$ profiles in Figures 8 and 11 are significant and reflect the fact that so long as the mean free path of the medium is finite, there will be corrections to the asymmetries of the resulting $f(v)$. These low-energy modifications are most nearly in response to local thermodynamic forces, as will be discussed in detail in paper 3, and are of the same sense as Chapman-Enskog theory would suggest.

Solar Rotation Effects

The asymptotically wrapped Archimedian spiral of the magnetic tubes of force in the plane of the ecliptic plays an important role in determining the nature of f^- in the extrathermal energy regime reported in the previous solutions. The arc length l along B scales (cf. (33)) as r^2 for large r in the ecliptic but only linearly with r over the magnetic poles of the sun. Thus the cumulative number of Coulomb 'collisions' is relatively enhanced in the ecliptic versus the polar regions by this geometrical hindrance of the guiding centers following the tubes of force. This situation may have an important impact on the nature of the magnitude of Coulomb backscattered extrathermals seen over the pole of the sun. Whether this implies a large skewness and resulting large heat flux on polar tubes of force depends on the electrostatic shielding of the interplanetary medium from the corona. The magnitude of this shielding is determined by the detailed polar coronal profiles of density, electron pressure, and waves. If the polarization potentials are very strong so as to support large asymptotic flows over the poles there may not be a substantial extrathermal population 'leaking' into interplanetary space. In this situation it may not be important for the value of the heat flux that cumulative Coulomb backscattering of extrathermals is weaker than it is in the ecliptic.

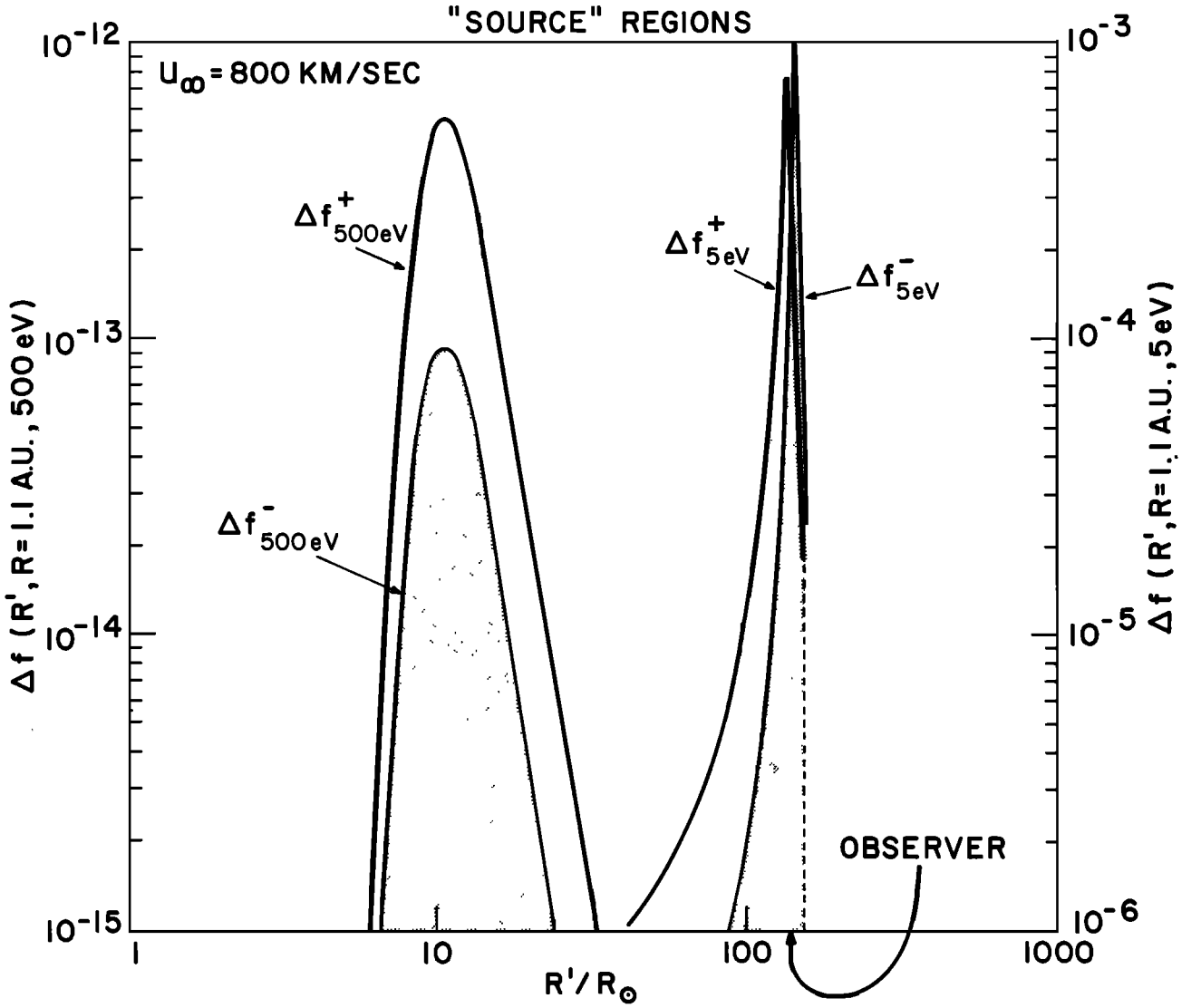

Fig. 12. Dominant spatial contributions to solution in Figure 11, same format as Figure 10, but for the solution shown in Figure 11. Note reduced scale for extrathermal contributions.

Remarks

The solutions for $f^{(1)}$ are not the fully self-consistent solution to the Coulomb scattering problem in the solar wind. These solutions indicate what type of modification the finite Coulomb mean free paths produce in the local distribution function and what forces and scales are important in the problem. We shall formulate and solve the more difficult fully self-consistent problem in paper 4 of this series.

7. Conclusions

We have shown that Coulomb collisions are substantial mediators of the interplanetary electron velocity distribution function. This is true for both the thermal distribution and the suprathermal populations. For the suprathermals the cumulative effects of Coulomb interactions take place on the scale of the heliosphere itself, whereas the thermal population's Coulomb interactions are numerous on the local scale (¼–½ AU) near the point of observation (1 AU). The suprathermal electron phase density at 1 AU is populated by electrons which most recently were members of collisional distributions very deep in the corona in or near the region (1–10 R_S) of the strong acceleration of the solar wind.

We have also shown that the properties of Coulomb collisions and the forces implied in the solar wind expansion, without benefit of wave-particle effects, can place a zone for a bifurcation of the electron distribution function deep in the corona. The site of this fractionation (1–10 R_S) is consistent with the result of extrapolating the radial profiles of T_c and T_h determined from Mariner 10 data reported by *Ogilvie and Scudder* [1978].

In the steady state the present considerations lead to a variety of predictions which can be tested against the growing body of electron data becoming available. Some of the more obvious relations implied in the model for an observer at a fixed radial position are the anticorrelation of local bulk speed with fractional extrathermal density, extrathermal differential temperature estimates, and heat flux density. In addition, the extrathermal differential temperature should be nearly independent of heliocentric distance within 1 AU owing to the small number of Coulomb momentum transfer 'collisions' and thus even fewer energy exchange 'collisions' between the corona and 1 AU.

We strongly emphasize the need to think of the transthermal and extrathermal electron kinetics in the solar wind on the

global scale because (1) the causes of insitu changes in properties of these electrons may not always be local ones, (2) nonlocal causes may affect different local parameters (e.g., speed, suprathermal population) in different ways, thereby inducing correlations in local measurements and the converse, and (3) observed local correlations in electron parameters do not imply local causal inerrelationships. The conventional transport question for solar wind electrons must be reposed to reflect the global character of the transthermal and suprathermal electrons which implement the various transport signatures.

By contrast, the subthermal electrons should in this picture reflect local cause and effect relationships. These electrons should be shaped by the local thermodynamic forces. Nevertheless, the thermals and suprathermals are Coulomb collisionally interacting locally. In steady state the thermal and suprathermal electrons observed at the same time were once members at different times of the (same) collisional equilibrium at the base of the same field line. Thus in varying degrees, the halo more, the core less, the subthermals and suprathermals retain a memory of having interacted with this same reservoir. We thus suggest that the nearly fixed ratio between T_e and $T_{extra} \sim T_h$ at 1 AU, for example, is a remnant of this fact. This is another example of a nonlocal factor inducing local correlations in observed parameters.

By considering the global effects of Coulomb collisions, we have shown that the distribution function for electrons similar to those reported can be reproduced in overall shape, skewness, and partition of phase density with energy. In particular, we have no difficulty in obtaining the backscattered portion of the extrathermal population (the 'halo'). The extrathermal population is a natural consequence of the evolution of a very hot, dense, inhomogeneous coronal plasma on open field lines.

To summarize, we should like to reemphasize the point made in the introduction: the observed 'overabundance' of higher-energy (suprathermal) electrons as judged by the local Maxwellian distribution of lower-energy (core) electrons is a direct consequence of the nonuniformity of the expanding medium of which the electrons are an intrinsic part. Expansion implies cooling and decrease in density as one moves along any open magnetic tube of force. This circumstance causes the Coulomb mean free path of sufficiently high-energy electrons to grow with distance to the point that it becomes comparable to or larger than the local scale length; this, in turn, renders the problem to be global (nonlocal) in character. The growth of the mean free path does not, however, imply that the effects of Coulomb collisions become negligible on a global scale. In fact, for the topology of magnetic fields at hand, the Coulomb collisions are never negligible, whatever the energy of the observed electron may be.

The electrostatic, magnetic, and gravitation fields combined with the action of Coulomb processes on global scale shape a non-Maxwellian distribution that, at first glance, appears to be composed of two distinct electron populations, thermal and suprathermal. Unlike the customary discussion of the origin of suprathermals [*Parker and Tidman,* 1958], we do not invoke Fermi or betatron equivalent energization, nor have we invoked shock acceleration, nor do we require leakage from closed coronal field lines as suggested by *Feldman et al.* [1975] to populate the extrathermal regime.

In conclusion, we would like to stress that the above described set of circumstances is not peculiar to our sun alone, but rather obtains in a great variety of (rotating) astrophysical objects. Any star (or, even perhaps some planets like Jupiter) that possesses an expanding ionized atmosphere with open magnetic field line topology should have electron distributions of the type observed in our solar system.

The above discussion should not be misconstrued as to indicate that the interactions of positive ions with waves are ruled out by this analysis. In fact, they may be of primary importance. Provided the magnetic turbulence invoked for the ions is laminar on the scale of the electron gyroradius, there will be no contradictions to the current work, since such variations would appear to make only minor path length modifications to $\delta S(R', R)$, without there being any significant electron-wave scattering interaction.

We believe that our results are sufficiently encouraging to warrant a more detailed and self-consistent formulation of the Coulomb scattering problem in the solar wind, which will be discussed in paper 4 of this series.

APPENDIX: DERIVATION OF (21)

Figure A1 depicts the arc length l versus time t history of an electron from an initial arc length l_m and time $t_<(l_m)$ until it returns to the same arc length l_m at a later time $t_>(l_m)$, having had one turning point ($dl/dt = 0$) at $(l^*, t^*(l^*))$ in the elapsed time. We define the contour C as the trajectory determined by the (assumed reversible) equations of motion which connects $(l_m, t_<)$ with $(l_m, t_>)$. We also define subcontours C_1 from $(l_m, t_<) \rightarrow (l^*, t^*)$ and C_2 from $(l^*, t^*) \rightarrow (l_m, t_>)$.

Clearly,

$$\oint_C dS = \oint_{C_1} dS + \oint_{C_2} dS \tag{A1}$$

The choice of subcontours is divided at (l^*, t^*) so that $l(t)$ is a one-one function on each subcontour. Therefore the contour integral can be made into ordinary integrals using the equation of motion

$$dl/dt'' = v_{\parallel}(l(t'', C)) \tag{A2}$$

or using the one-one nature of $l(t)$ on C_1, C_2,

$$\frac{dl}{v_{\parallel}(l(t''), C_1)} = dt'' \qquad (C_1 \tag{A3a}$$

$$\frac{dl}{v_{\parallel}(l(t''), C_2)} = dt'' \qquad (C_2 \tag{A3b}$$

Equation (A1) may be rewritten as

$$\oint_{t_<(l_m)}^{t_>(l_m)} dS \equiv \Delta S_{m,m+1} \equiv \delta_{m,*} + \delta_{*,m+1} \tag{A4a}$$

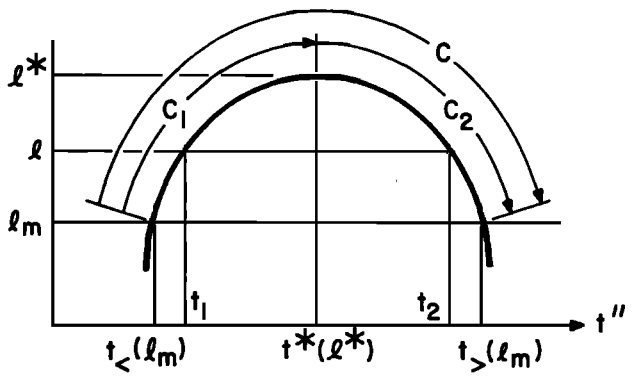

Fig. A1. Schematic diagram to assist in deriving (21). Note that script els in the figure have been set in the text as lower case italic els.

where

$$\delta_{m,*} = \oint_{c_1} dS = \int_{t_m}^{t_*} \frac{dl}{\tau[t''(l(C_1)), \mathbf{w}(l)]v_{\|}(l(C_1))}$$
$$\delta_{*,m+1} = \oint_{c_2} dS = \int_{t^*}^{t_m} \frac{dl}{\tau[t''(l(C_2)), \mathbf{w}(l)]v_{\|}(l(C_2))} \quad \text{(A4b)}$$

Let t_1 be any time on contour C_1 for the particle to be at arc length l on a trajectory with given turning point as indicated in Figure A1. By the one-one nature of the contour C_2 there is a unique time t_2 when the same particle following contour C_2 is at l. If, as we have assumed, the scattering is elastic and the external forces conservative, we have the relationship

$$v_{\|}(l(C_1)) = -v_{\|}(l(C_2)) \quad \text{(A5)}$$

The collision time τ depends on the density n and temperature of the 'target' particles. By the time stationarity assumption $n(r(l), t_1)$ equals $n(r(l), t_2)$, a similar relation holds between the temperatures at the same place at different times. The collision time also depends only on the 'test' particle's proper frame speed $|\mathbf{w}|$, where $\mathbf{w} = \mathbf{v} - \mathbf{u}$, $\mathbf{u}$ being the bulk velocity of the targets. Since $\mathbf{w} \simeq \mathbf{v}$ for electrons in the solar wind, then $\tau(+v_{\|}, l)$ is essentially $\tau(-v_{\|}, l)$. Therefore

$$\delta_{*,m+1} = \int_{t^*}^{t_m} \frac{dl}{\tau(t''(l(C_2)), |\mathbf{w}(l(C_2))|)(-v_{\|}(l(C_1)))}$$
$$\simeq \int_{t_m}^{t_*} \frac{dl}{\tau(t''(l(C_1)), |\mathbf{w}(l(C_1))|)(v_{\|}(l(C_1)))}$$
$$\simeq \delta_{m,*}$$

Therefore

$$\Delta S_{m,m+1} \equiv \delta_{m,*} + \delta_{*,m+1} \simeq 2\delta_{m,*}$$

which is (21).

Acknowledgments. One of us (J.S.) would like to acknowledge discussions and/or manuscript comments by M. Acuña, L. Burlaga, A. Klimas, K. Ogilvie, V. Pizzo, and E. Sittler at NASA/Goddard Space Flight Center, R. Boswell, E. Marsch, W. Pilipp, and H. Rosenbauer while a guest at Max-Planck-Institute für Extraterrestriche Physik, Garching, West Germany, and the interest of H. S. Bridge of the Massachusetts Institute of Technology. We appreciate the comments of both referees.

The Editor thanks A. J. Hundhausen and M. Schulz for their assistance in evaluating this paper.

REFERENCES

Acuña, M., and Y. C. Whang, A two region model of the solar wind including azimuthal velocity, *Astrophys. J., 203,* 720, 1976.

Bame, S. J., J. R. Asbridge, W. C. Feldman, and P. D. Kearney, The quiet corona: Temperature and temperature gradient, *Solar Phys., 35,* 137, 1974.

Belcher, J. W., Alfvénic wave pressures and the solar wind, *Astrophys. J., 168,* 509, 1971.

Bhatnagar, P. L., E. P. Gross, and M. Krook, A model for collision processes in gases, I, Small amplitude processes in charged and neutral one component systems, *Phys. Rev., 94*(3), 511, 1954.

Brandt, J. C., and J. P. Cassinelli, Interplanetary gas, 11, An exospheric model of the solar wind, *Icarus, 5,* 47, 1966.

Chamberlain, J. W., Interplanetary gas, 2, Expansion of a model solar corona, *Astrophys. J., 133,* 47, 1960.

Durney, B. R., and A. J. Hundhausen, The expansion of a low-density corona: a one-fluid model with magnetically modified thermal conductivity, *J. Geophys. Res., 79,* 3711, 1974.

Durney, B. R., and G. W. Pneuman, Solar interplanetary modeling: 3-D solar wind solutions in prescribed non-radial magnetic field geometries, *Solar Phys., 40,* 461, 1975.

Feldman, W. C., M. D. Montgomery, J. R. Asbridge, S. J. Bame, and H. R. Lewis, Interplanetary heat conduction—Imp 7 results, in *Solar Wind Three,* edited by C. T. Russell, Institute of Geophysics and Planetary Physics, University of California Press, Los Angeles, 1974.

Feldman, W. C., J. R. Asbridge, S. J. Bame, M. D. Montgomery, and S. P. Gary, Solar wind electrons, *J. Geophys. Res., 80*(31), 4181, 1975.

Feldman, W. C., J. R. Asbridge, S. J. Bame, J. T. Gosling, and D. S. Lemons, Characteristic electron variations across simple high-speed solar wind streams, *J. Geophys. Res., 83,* 5285, 1978.

Forslund, D. W., Instabilities associated with heat conduction in the solar wind and their consequences, *J. Geophys. Res., 75,* 17, 1970.

Gary, S. P., W. C. Feldman, D. W. Forslund, and M. D. Montgomery, Heat flux instabilities in the solar wind, *J. Geophys. Res., 80*(31), 4197, 1975.

Griffel, D. H., and L. Davis, The anisotropy of the solar wind, *Planet. Space Sci., 17,* 1009, 1969.

Gross, E. P., and M. Krook, A model for collision processes in gases: Small amplitude oscillations of charged two-component systems, *Phys. Rev., 102,* 3, 1956.

Hartle, R. E., and P. A. Sturrock, Two-fluid model of the solar wind, *Astrophys. J., 151,* 1155, 1968.

Hundhausen, A. J., Direct observations of solar wind particles, *Space Sci. Rev., 8,* 690, 1968.

Jockers, K., Solar wind models based on exospheric theory, *Astron. Astrophys., 6,* 219, 1970.

Kopp, R. A., and F. Q. Orrall, Models of coronal holes above the transition region, in *Coronal Holes and High Speed Wind Streams,* edited by J. B. Zirker, Colorado Press, Boulder, 1977.

Lemaire, J., Kinetic vs. hydrodynamic models, paper presented at the Conference on Highlights in Solar Physics, (French) Nat. Center for Sci. Res., Toulouse, France, March 1978.

Lemaire, J., and M. Scherer, Kinetic models of the solar wind, *J. Geophys. Res., 76,* 7479, 1971.

Lemaire, J., and M. Scherer, Kinetic models of the solar and polar winds, *Rev. Geophys. Space Phys., 11*(2), 427, 1973.

Maxson, C. W., and G. S. Vaiana, Determination of plasma parameters from soft X-ray images for coronal holes (open magnetic configuration) and coronal large scale structures (extended closed field configurations), *Astrophys. J., 215,* 919, 1977.

Montgomery, M. D., Average thermal characteristics of solar wind electrons, Solar Wind, *NASA Spec. Publ. 308,* 208, 1970.

Montgomery, M. D., S. J. Bame, and A. J. Hundhausen, Solar wind electrons: Vela 4 measurements, *J. Geophys. Res., 73*(15), 4999, 1968.

Neugebauer, M., and C. W. Snyder, Mariner 2 measurements of the solar wind, in *The Solar Wind, JPL Tech. Rep. 32-630,* edited by R. J. Mackin and M. Neugebauer, Pergamon Press, New York, 1966.

Ogilvie, K. W., and J. D. Scudder, The radial gradients and collisional properties of solar wind electrons, *J. Geophys. Res., 83,* 3776, 1978.

Ogilvie, K. W., J. D. Scudder, and M. Sugiura, Electron energy flux in solar wind, *J. Geophys. Res., 76*(34), 8165, 1971.

Parker, E. N., Kinetic properties of interplanetary matter, *Planet. Space Sci., 9,* 461, 1962.

Parker, E. N., *Interplanetary Dynamical Processes,* John Wiley, New York, 1963.

Parker, E. N., and D. A. Tidman, Suprathermal particles, *Phys. Rev., 111*(5), 1206, 1958.

Pines, D., and D. Bohm, A collective description of electron interactions, II, Collective vs. individual particle aspects of interactions, *Phys. Rev., 85*(2), 338, 1952.

Rawls, J. W., M. S. Chu, and F. L. Hinton, Transport properties of a toroidal plasma of intermediate to high collision frequencies, *Phys. Fluids, 18*(9), 1160, 1975.

Reif, F., *Fundamentals of Statistical and Thermal Physics,* McGraw-Hill, New York, 1965.

Rosenbauer, H., H. Miggenreider, M. Montgomery, and R. Schwenn, Preliminary results of the Helios plasma measurements, in *Physics of Solar Planetary Environments,* edited by D. Williams, p. 319, AGU, Washington, D. C., 1976.

Rosenbauer, H., R. Schwenn, E. Marsch, B. Meyer, H. Miggenreider, M. D. Montgomery, K. H. Mühlhäuser, W. Pilipp, W. Voges, and S. M. Zink, A survey on initial results of the Helios plasma experiment, *J. Geophys., 42,* 561, 1977.

Rosenbluth, M., W. M. MacDonald, and D. L. Judd, Fokker-Planck equations for an inverse-square force, *Phys. Rev., 107,* 1, 1957.

Rossi, B., and S. Olbert, *Introduction to the Physics of Space*, McGraw-Hill, New York, 1970.

Scudder, J. D., Comments, Solar Wind, *NASA Spec. Publ. 308*, 211, 1970.

Singer, C. E., and I. W. Roxburgh, The onset of microinstability and its consequences in the solar wind, *J. Geophys. Res.*, *82*(19), 2677, 1977.

Sittler, E. C., Study of the electron component of the solar wind and magnetospheric plasma, Ph.D. dissertation, Mass. Inst. of Technol., Cambridge, Feb. 1978.

Sittler, E. C., and S. Olbert, Radial profiles of the solar wind velocity, temperature, and heat flux vector based on the empirical density profile and empirical magnetic field line topology (abstract), *Eos Trans. AGU*, *58*(6), 484, 1977.

Spitzer, L., Jr., and R. Härm, Transport phenomena in a completely ionized gas, *Phys. Rev.*, *89*, 977, 1953.

(Received September 22, 1978;
revised February 6, 1979;
accepted February 6, 1979.)